GIS-BASED GROUNDWATER POTENTIAL MAPPING AND RECHARGE ESTIMATION: A CASE STUDY IN MELKAODA WATERSHED RIFT VALLEY LAKES BASIN, OROMIA, ETHIOPIA

M. Sc. THESIS

ADEM BUTA DEKEBO

HAWASSA UNIVERSITY, HAWASSA, ETHIOPIA

JUNE, 2021

GIS BASED GROUNDWATER POTENTIAL MAPPING AND RECHARGE ESTIMATION: A CASE STUDY IN MELKAODA WATERSHED RIFT VALLEY LAKES BASIN, OROMIA, ETHIOPIA

ADEM BUTA DEKEBO

A THESIS SUBMITTED TO THE

FACULTY OF BIO-SYSTEMS AND WATER RESOURCE ENGINEERING

DEPARTMENT OF WATER RESOURCE AND IRRIGATION ENGINEERING

HAWASSA UNIVERSITY INSTITUTE OF TECHNOLOGY

SCHOOL OF GRADUATE STUDIES

HAWASSA UNIVERSITY

HAWASSA, ETHIOPIA

IN PARTIAL FULFILLMENT OF THE REQUIREMENTS FOR THE DEGREE OF MASTERS OF SCIENCE IN WATER RESOURCE AND IRRIGATION ENGINEERING

(SPECIALIZATION: IRRIGATION AND DRAINAGE ENGINEERING)

SCHOOL OF GRADUATE STUDIES

HAWASSA UNIVERSITY

ADVISORS APPROVAL SHEET

This is to certify that the thesis entitled "GIS BASED GROUNDWATER POTENTIAL MAPPING AND RECHARGE ESTIMATION: A CASE STUDY IN MELKAODA WATERSHED, RIFT VALLEY LAKES BASIN, OROMIA, ETHIOPIA" submitted in partial fulfillment of the requirements for the degree of masters with specialization in water resource engineering and management, Department of the water resource and irrigation engineering, and has been carried out by ADEM BUTA DEKEBO ID NO. PGIrDrR/0001/11, under our supervision. Therefore, we recommend that the student has fulfilled the requirements and hence hereby can submit the thesis to the department.

Major Advisor: Tewodros Assefa (Ph.D.) _____ _____

Signature Date

Co-Advisor: Teshale Taddesse (M.sc.) _____ _____

Signature Date

ACKNOWLEDGEMENT

Above all and for the most, my praise and thanks go to the almighty Allah who enables me to perform things through his strengthening arm and guides me to the complete success that has been predestined by him. My deepest heartfelt gratitude and appreciation is for my Major Advisor Dr. Tewodros Assefa, Co-Advisor Teshale Taddesse, and Ayelew Shura for their invaluable guidance and consultation through my research studies by spending most of their time to give me advice.

I extend my appreciation to all organizations and individuals who helped me in my study. First I would like to thank Dilla University for its financial support. The last but not least, I would like to acknowledge the Ministry of Water, irrigation and Electricity of Ethiopia, and the Ethiopian Meteorological Agency for giving me the necessary data. Finally, I appreciate my family who supported and strengthened me morally.

DECLARATION

I hereby declare that this M.Sc. thesis is my original work and has not been presented for a degree in any other university, and all sources of material used for this thesis have been duly acknowledged.

Name Adem Buta

Signature: _____

LIST OF ABBREVIATIONS AND ACRONYMS

M.A.S.L	Meters above Sea Level
AHP	Analytical Hierarchy Process
AOI	Area of Interest
ASCII	American Standard Code for Information Exchange
CR	Consistency Ratio
DEM	Digital Elevation Model
DMC	Double Mass Curve
ERDAS	Earth Resource Data Analysis System
ET_i	Actual evapotranspiration from impervious surface
ET_O	Actual evapotranspiration from open water
ETs	Actual evapotranspiration from bare soil
ET_V	Actual evapotranspiration from the vegetation
FAO	Food and Agriculture Organization
GIS	Geographical Information System
GPZM	Groundwater Potential Zone Mapping
IDW	Inverse Distance Weight
JMG	Journal of Management and Governance.
LANDSAT	Land Space Application Technology
LULC	Landuse/Land Cover
LULCC	Landuse/Land Cover change

MCDA	Multi-Criteria Decision Analysis
MER	Main Ethiopian Rift Valley
MoWIE	Ministry of Water Irrigation and Energy
NMA	National Meteorological Agency
OLI	Operation Landsat Imager
OUPI	Oromia Urban Planning Enterprise
PET	Total Potential Evapotranspiration
RS	Remote Sensing
SAGA	System for Automated Geoscientific Analyses
SOE	Survey of Ethiopia
SRTM	Shuttle Radar Topography Mission
SWL	Static Water Level
TBL	Table of Values
USDA	United State Department of Agriculture
USGS	United States Geological Survey
WETSPASS	Water and energy transfer between soil, plants, and atmosphere under quasi-steady-state
WIOA	Weight Index Overlay Analysis
WOA	Weighted Overlay Analysis
TPI	Topographic Position Index
GWD	Groundwater Depth

TABLE OF CONTENTS

LIST OF TABLES

LIST OF FIGURES

LIST OF APPENDICES

ABSTRACT

The groundwater potential zones of the Melkaoda Watershed were demarcated with the help of remote sensing and Geographic Information System (GIS) techniques. The parameters that were considered for identifying the groundwater potential zone like geology, slope, drainage density, geomorphic units, and lineament density were generated from satellite data and they were then integrated with weighted overlay in ArcGIS. Suitable ranks were assigned for each category of these parameters and weight factors were decided for them based on their capability to store groundwater using AHP approach and then the groundwater potential zones were classified into four categories as very low, low, high & very high. In addition, the groundwater recharge was estimated with the help of the WetSpass model using water balance approach. The parameters considered for this case generally included three types: hydro-meteorological (rainfall, temperature, wind speed, PET, and GWD), bio-physical (soil, landuse, topography, and slope), and attribute lookup (soil lookup, landuse lookup, and rain day lookup) tables. All the hydro-meteorological parameters were interpolated in ArcGIS for grid map preparation of each parameter and the prepared grid map was converted to ASCII file format for the effective model run. The model performance was checked through calibration and the obtained groundwater recharge result ranges 0.45 to 65.5 mm/year with the mean value of 32.87 mm/years and 3.4% contributed to groundwater as recharge. finally, the changes in groundwater recharge between two simulation period was stated again with help of WetSpass model using the LULC images of 1989 and 2018 to quantify the impacts of the LULCC. The parameters used for this analysis were the same as those used for groundwater recharge estimation except for the satellite image of 1989 and the LULCC analysis depicted that there was the expansion of built-up land and agricultural land. Agricultural land and built-up land were increased by 0.046, 2.56 rate per a year from 1989 to 2018 respectively. This paper finalized that there was access to the groundwater potential in the Melkaoda Watershed and this could overcome the water scarcity challenging the community in and around the area. The recharge which has been the main source of groundwater is decreasing from time to time as the result of this paper is indicating. Thus, to get sustainable groundwater potential, the recharge has to be well treated by increasing groundwater recharge.

Keywords: GIS, WetSpass model, Groundwater recharge, Melkaoda watershed, and LULCC

1. INTRODUCTION

1.1 Background

Water resource, which is the backbone and crucial element of life, is needed in sufficient quantity and quality to meet the increasing demand for domestic, agricultural, and industrial processing operations (Fenta et al., 2014; Shanableh and Merabtene, 2015; Arefayne et al.., 2015). Mostly, water resource is found as surface water and groundwater forms, surface water is not a reliable source as it is prone to seasonal fluctuations and susceptible to contamination through anthropogenic activities such as point, non-point pollution sources and biological pollutions (Fenta et al., 2014). However, groundwater is more suitable in quantity, readily available, and is naturally protected from direct contamination by surface anthropogenic activities (Fenta et al., 2014). It is the largest reservoir of liquid freshwater on the planet and is critical for sustaining life on earth, as it is used to satisfy different human and environmental needs (Zomlot et al., 2015).

Groundwater is the most valuable natural resource, which supports human health, economic development, and ecological diversity. Because of its several inherent qualities, it has become an immensely important and dependable source of water supplies in all climatic regions including both urban and rural areas of developed and developing countries (Waikar,2014). Groundwater is a form of water occupying all the voids within a geological stratum. Water-bearing formations of the earth's crust act as conduits for transmission and as reservoirs for storing water. The groundwater occurrence in a geological formation and the scope for its exploitation primarily depends on the formation of porosity, high relief, and steep slopes impart higher runoff, while topographical depressions increase infiltration. An area of high drainage density also increases surface runoff compared to a low drainage density area. Surface water bodies like rivers, ponds, etc., can act as recharge zones (Murugesan et al., 2012). In many arid regions, aquifers are the only water source (Mata-González et al., 2012). Groundwater has become an indispensable natural resource for human survival in the context of changing climate and population growth (Panda and Kumar, 2011).

Groundwater recharge is the entry into the saturated zone of water made available at the water table surface together with the associated flow away from the water table within the saturated zone and regional groundwater models used for analyzing groundwater systems (infiltration–

discharge relations) are often steady state and, therefore, need long-term average recharge input (Freeze, 1969). WetSpass was built as a physically-based methodology for estimation of the long term average, spatially varying, water balance components such as surface runoff, actual evapotranspiration, and groundwater recharge, and the model was especially suitable for studying the effects of landuse changes on the water regime in a basin (Adnan et al., 2010).

It is important to recognize and understand land cover (biophysical attributes of the earth's surface) and landuse (human purpose or intervention applied to these attributes) changes as the major ecological processes affecting and that are affected by the dynamic interaction of ecosystems (Ricca and Guagliardi, 2015) and in turn, the impact of the hydrological responses of a catchment by altering the partitioning of precipitation into different components of the hydrological cycle, as interception, infiltration, runoff, evapotranspiration, and groundwater recharge rate (Aduah, 2015).

The geology of Ethiopia provides usable groundwater and good transmission of rainfall to recharge aquifers which produce spring and feed perennial rivers. In many parts of the country, groundwater is an important source of domestic and industrial water use. With the understanding of the nature of the distribution of the country, it was estimated the total groundwater reserve of the country as 185BMC, which is distributed in an area of 924,140 km^2 made of Sedimentary, Volcanic, and Quaternary rocks (Berhanu., 2014).

Ethiopia has also the groundwater potential, ranging from 2.6 to 2.65 billion m^3, and an estimated 122 billion m^3 of annual runoff water (Awulachew et al., 2007). However, <5% of the surface water potential is currently utilized by the people, and groundwater is a potential, but untouched resource (Tesfamichael et al., 2013).

Understanding seasonal, monthly, and annual variations of the water resources, especially runoff, evapotranspiration, and recharge, is necessary for efficient and sustainable management of groundwater (Obuobie, et al., 2008). Since groundwater resources are sensitive functions of climatic factors, geological formation, topography, soil properties, and land-use types (Dragoni & Sukhija, 2013), a detailed understanding of watershed physical and biological characteristics are important

Accurate quantification of groundwater resources involves identification of hydrological and biophysical characteristics of the watershed. Regional groundwater models used for analyzing groundwater systems (infiltration– discharge relations) are often steady state and, therefore,

need long-term average recharge input. On the other hand, the spatial variation in the recharge due to distributed land-use, soil type, slope, etc., can be significant and should be accounted for regional groundwater models. Hence, the WetSpass was built as physically-based methodology for estimation of long-term average, spatially varying, water balance components: surface runoff, actual evapotranspiration, and groundwater recharge. It was built upon the foundations of the time dependent spatially distributed water balance model WetSpa (Batelaan et al., 1996, Wang, 1997).

From a volume perspective, most water used in the Melkaoda Watershed is appropriated from groundwater. Since the rainfall of the watershed is seasonal, most of the time, the tributaries, and the main river have been shown scarcity. Hence, this forces the local communities to use subsurface water not only for drinking but also for domestic uses and in some cases for irrigation purpose. Though this groundwater is recharged from precipitation, utilization of this resource is going on without a basic understanding of the recharge amount and its areal distribution as well as the temporal and spatial variation of the other water balance components which creates a critical problem for its management in the watershed. In this paper groundwater recharge, surface runoff and evapotranspiration are estimated for the Melkaoda watershed using WetSpass modeling method.

1.2 Statement of the Problem

Groundwater potential was under a great problem due to over-extraction, quality degradation, and unbalanced utility of sustainable groundwater use at all levels (Giordano, 2009).

Access to safe drinking water becomes a problem in many regions of the world particularly in the dryland of developing countries because of high growth and competing demand for the resource (Esayas and Gebeyehu, 2018). Over the years, the growing importance of groundwater based on an increasing need has led to unscientific exploitation of groundwater creating a water stress condition and this alarming situation calls for a cost and time-effective technique for proper evaluation of groundwater resources and management planning (Waikar and Aditya, 2014). Currently, groundwater is gaining more attention due to drought problems, rural water projects, supply, irrigation and the low cost of development it requires. Despite the extensive research and technological advancement, the study of groundwater has remained riskier, as there is no direct method to facilitate observation of water below the surface and only infer its

presence or absence indirectly by studying the geological and surface parameters (Waikar and Aditya, 2014). It is a scarce, crucial, and multifunctional natural resource found on the planet and the demand for freshwater is increasing worldwide as a result of urbanization, economic, and population growth (Karimi and Bastiaanssen 2015). Because of its scarcity, proper planning and management of such resources in terms of distribution, management, utilization, and environmental functions are significant for optimizing resource use sustainably (Karimi and Bastiaanssen 2015). A groundwater-developing program requires a large volume of data from various sources. Hence, identification and quantization of these features are important for generating a groundwater potential model of a study area (Waikar and Aditya, 2014).

Shashamane town is one of the fastest growing towns in population among the cities of Ethiopia which is found in this watershed and the increase of the population was exposing load on the available groundwater resources in the area. Water scarcity was the main problem in the study area as highly used for different purposes by different users even though there was no enough information about the available water source such as groundwater potential and recharge on this specific watershed for wise and sustainable utilization and proper management of the limited groundwater resources. In this area getting potable water was more challenging and it was inviting the people for the unexpected cost to get water. So, to overcome these problems giving more attention to groundwater seems the only solution in this area as the surface water is becoming scarcer. As existing information indicates, there was no study conducted concerning the groundwater potential in this area and this situation was challenging the policy and decision-maker from wise and sustainable utilization of water resources. So this research was conducted to identify the best possible solution for solving the problems concerning the study area.

Quantification of the recharge rate is a prerequisite for the efficient and sustainable management of groundwater (Obuobie et al., 2012). Facing global environmental change including climate change, landuse change, and eventually adaptation processes, it is essential to assess the impacts of all changes on the groundwater recharge and resources (Stoll, 2012). Thus the determination of groundwater recharge has shifted from a basic problem to an urgent and fundamental issue in hydro-geologic research for sustainable development of groundwater (Rwanga, 2013).

Landuse affects groundwater resources through changes in recharge and by changing demands for water (Fan, 2015: Lerner and Harris, 2009: Tetzlaff et al., 2007). The impact of urbanization on groundwater has a major concern to most urban areas over the past few decades, and in

particular, to those involved in groundwater quantity and qualitative studies (Morris et al.., 1994; Salvadore et al., 2015; Schirmer et al., 2013). The increased impervious area has been a major factor in contributing to decreased infiltration, which results in decreasing groundwater storage. So, urbanization was the major issue in the study area that was increasing at a high rate, and that extensively affecting groundwater recharges.

1.3 Objective

1.3.1 General Objective

The general objective of the study was to map groundwater potential zones and estimate groundwater recharge in the Melkaoda Watershed.

1.3.2 Specific Objective

The specific objectives in this study were:

- To identify the potential zones of the area by using GIS and remote sensing.
- To quantify the groundwater recharge by using the WetSpass modal.
- To assess the impact of changes in landuse/land cover on groundwater recharge in the study area.

1.4 Research Question

- Where? A very low, low, moderate, high, and very high groundwater potential in the study area is found?
- How much quantity of rainfall has been recharging the groundwater?
- To what extent the change in landuse/land cover impact groundwater recharge in the study area?

1.5 Significance of the study

The knowledge of groundwater potential of watershed allows local governments, policymakers, and any concerned body to formulate and implement effective and appropriate planning activity for water resources development works in the watershed. The study pointed out, the method of potential mapping, determining groundwater recharge, and evaluating impacts of landuse/land cover on studied watershed using geographical information system and WetSpass model respectively.

1.6. Scope of the study

The scope of this research is limited to map groundwater potential, recharge estimation, and impacts of landuse changes on groundwater recharge at Melkaoda Watershed. Since it is desirable to limit the scope of the problem to management objectives.

2. LITERATURE REVIEW

2.1. Water resources

The World's total water resource estimation is about 1.36×10^8 M ha-m. Of these global water Resources, about 97.2% are saltwater mainly in oceans, and only 2.8% are available as fresh water at any time on the planet earth. Out of this 2.8% of fresh water, about 2.2% is available as surface water and 0.6% as groundwater. Even out of this 2.2% of surface water, 2.15% is fresh water in glaciers and icecaps, and only of the order of 0.01% is available in lakes and streams, the remaining 0.04% being in other forms. Out of 0.6% of stored groundwater, only about 0.25% can be extracted economically with the present drilling technology the remaining being at greater depths (Raghunath, 2006).

Very little of the Earth's abundant water is accessible and suitable for human needs. This is especially true in Africa. At the continental level, Africa's 3931 km^3 of renewable water resources represent around 9% of the world's total freshwater resources. Africa is the world's Second-driest continent, after Australia, but also the world's most populous continent after Asia (UNEP, 2010).

2.2 Groundwater potential

There were different definitions given to groundwater potential by different authors at different times. According to (Rashman, 2016), groundwater is the most important natural resource found beneath the earth's surface stored in a void space of geological stratum used in economic development, domestic life, and any ecological diversity. Also, he concludes the occurrence and flows system of groundwater is depends on geological characteristics of its porosity and permeability and the formation of landforms such as high mountains, rift valleys, and flat areas, and the role of landform on surface runoff and infiltration to the ground. Groundwater is the subsurface water that occurs beneath the water table in the soils and geologic formations that are fully saturated (Freeze & Cherry., 1979).

Groundwater use has fundamental importance to meet the rapidly expanding urban, industrial and agricultural water requirement, especially in arid areas where surface waters are scarce and seasonal. Uneven distribution of surface water resources resulted in an increased emphasis on the development of groundwater resources. An important objective of most groundwater studies is to make a quantitative assessment of the groundwater resources in terms of the total volume

of water stored in an aquifer or long-term average recharge. Groundwater recharge is determined largely as an imbalance at the land surface between precipitation and evaporative demand. When precipitation exceeds evaporative demand by an amount sufficient to replenish soil water storage, further excess flows deeper into the ground and arrives at the water table as recharge.
(Waikar and Nilawar, 2014) have conducted the research on Identification of Groundwater Potential Zone using Remote Sensing and GIS Technique in Parbhani district of Maharashtra with help of Analytical Hierarch process and finally, they found that the groundwater potential zones are classified into five categories like very poor, poor, moderate, good & excellent. (Murugesan et al., 2012) have carried out groundwater study in the Dindigul district of kodaikanal hill, which was a mountainous terrain in the Western Ghats of Tamilnadu and groundwater potential zones have been demarcated with the help of remote sensing and Geographical information (GIS) techniques. All thematic maps are generated using the resource data and Inverse distance weight (IDW) model is used in GIS data to identify the groundwater potential of the study area. For the various geomorphic units, weight factors were assigned based on their capability to store groundwater.

2.3 Groundwater recharge

Depending on rainfall intensity, temperature, and ground surface cover, the precipitated water is subjected to various processes such as interception, evaporation, and surface runoff. A portion of the water may also infiltrate into the soil. The remaining water will continue percolating deeper into the soil column, eventually becoming groundwater recharge when crossing the water table into the saturated groundwater zone (Deng et al.., 2015). Groundwater recharge is the percolation/ infiltration of water from unsaturated zone to saturated zone through porosity and permeability of the earth materials above the water table and finalizes precipitation, infiltration/ percolation of the surface water to the subsurface influenced by geology and geomorphology (Rajaveni et al.., 2015). Recharge may occur naturally from precipitation, rivers, canals, lakes, as man-induced phenomena (irrigation, urban recharge). Recharge can be instantaneous, event, season, year, historical or geologic time.
(Meresa and Taye, 2018) have conducted research on estimation of groundwater recharge using GIS-based WetSpass model for Birki watershed, the eastern zone of Tigray, Northern Ethiopia and they have found that, summer (rainy season) recharge ranges from 0 to 41.09 mm/year with

mean value of 24.1 mm/year (96.5%), winter (dry season) recharge ranges from 0 to 1.9 mm/year with mean value of 0.8 mm/year (3.5%) and yearly recharge ranges from 0 to 42.6 mm/year with mean value of 24.9 mm/year. Ten years of mean annual precipitation 573 mm contributed to 7.4% as recharge to the groundwater, 7.1% of surface runoff and 85.5% lost as evapotranspiration.

2.4 Impacts of landuse/land cover on groundwater recharge

Groundwater is intimately connected with the landscape and landuse that it underlies and most of the landscape and is vulnerable to the anthropogenic activities on the land surface above. Landuse affects groundwater resources through changes in recharge and by changing water demands (Fan, 2015: Harris,2009: Tetzlaff,2007). Therefore, the rapid economic development and the accelerated urbanization in recent decades have resulted in the serious degradation of water resources (Su et al., 2015) via urbanization, industrialization, and intensive agriculture that result in rapid landscape change with the loss of ecological capacities (Ricca and Guagliardi, 2015). Human activity is one of the major driving forces leading to changes in land cover characteristics and subsequently hydrologic processes (Bonansea, 2016).

The increased impervious area has been a major factor in contributing to decreased infiltration, which results in increased surface water storage. The large pressure of the growing population increased demands for food, fodder, and fuel combined with industrial activities have essentially led to rapid change in landuse patterns in developing countries. Information on the rate and kind of change in the land resources is essential for proper planning, management, and regularizing the use of such resources. The landuse information is needed in the analysis of environmental processes and problems.

2.5 Groundwater in Ethiopia

Ethiopia is endowed with a substantial amount of water resources. The country is divided into 12 river basins; 9 of which are wet river basins; 1 lake basin; and the remaining 3 are dry river basins, with no or insignificant flow out of the drainage system. Almost all of the basins radiate from the central plateau of the country that separates into two due to the Rift Valley. Basins drained by rivers originating from the mountains west of the Rift Valley flow toward the west into the Nile River basin system, and those originating from the Eastern Highlands flow toward

the east into the Republic of Somalia. Rivers draining in the Rift Valley originate from the adjoining highlands and flow north and south of the uplift in the center of the Ethiopian Rift Valley (Melesse et al, 2013).

(Tamiru, 2006) Has done on the Groundwater occurrence in Ethiopia and described the most important factors governing the groundwater flow and storage in volcanic rocks. In addition, he summarizes that the variation in mineralogy, texture, and structure of volcanic rocks cause the variation of the water-bearing capacity of the area. (Kebede, 2010) conducted on the Groundwater occurrence in Ethiopia, partly he divided the source of groundwater recharge in Ethiopia under flood recharge, wadi flood recharge, rainfall recharge, and mountain block recharge, runoff from graben and summarize the water isotope is the evidence. (Yitbarek, 2012) Describe type and distribution of lithology in Ethiopia and they categorize sedimentary and Mesozoic sandstone to the southern, karstic rocks to eastern and southeastern, quaternary volcanic rocks and unconsolidated sediments in the rift valley and low land depression area, fractured intrusive rocks, old Precambrian rocks, and metamorphic rocks to the western part of Ethiopia and their aquifer characteristics. In addition to the above authors, (Pavelic, 2012) conducted on groundwater availability and use in the sub-Sahara African country review of fifteen countries. He summarizes that the hydrological conditions of sub-Sahara Africa are the major controller of groundwater more than other countries and categorizes the hydrological aquifers parameters of sub-Saharan into crystalline basement complex rock, consolidated sedimentary rock, unconsolidated sedimentary rock, and volcanic rocks. Although, (Adetunj and Odetokun, 2011) conducted Water balance of upper Awash River basins based on the satellite-derived data /Remote sensing data on his MSc thesis, understanding the spatial variations of water balance components of upper Awash River basins will provide full information for the management surface and groundwater. The geology of the main Ethiopia rift valley (MER) is very complex, which is difficult to describe the hydrology of the area because of variability and lateral discontinuity of volcanic rocks (Ernesto et al.., 2015).

Melkaoda was one of the Central Rift Valley Lakes Basin, which is found in the southern part of Oromia regions within the main Ethiopian rift valley (MER). Concerning this area, no longer reports were done in previous. Specially relating to groundwater, there were no reports that are done by different researchers on this area.

2.6 Factors affecting groundwater potential and recharge

Groundwater potential and recharge were affected by different factors that control/facilitate this process according to different previous works. As discussed by (Prasad et al.., 2008) on deciphering of the ground potential zone in hard rock water through the application of GIS. Partly he discussed Lithology, geomorphology, lineament, slope, soil, drainage pattern, landuse, and rainfall.

Finally, he summarized that the above parameters are very important factors in groundwater potential mapping and recharge determination. (Annesh and Paresh, 2015) Studied origin of occurrence and movement location of groundwater by using remote sensing data based on indirect analysis of directly observable terrain features like geological structures, geomorphology, Landuse/land cover, Slope, Rainfall, drainage density, and lineaments, Water bearing capacity of the area.

Drainage density

Drainage is one of the factors which play the important role in groundwater potential zone delineation. They are the reflection of the rate that precipitation infiltrated compared to surface runoff. Where rocks of the study area are highly permeable, infiltration to groundwater is high, and less water is transported in rivers as surface water; but where rocks of the study area have low permeability there is little infiltration and more surface water runoff. Low drainage density is therefore related to higher recharge and results in higher groundwater potential (Thangarajan., 2007). The drainage density is high in the plateau and escarpment and very low in the rift floor (Ayenew T., 1998). The high ranks are given to low drainage density due to more infiltration (Nilawar P. & Waikar M.L, 2014).

Lineament density

Lineaments are straight linear elements visible at the Earth's surface as significant “lines of landscape” (Hobbs, 1904). These are primarily a reflection of discontinuities on the Earth’s surface caused by geological or geomorphic processes (Clark & Wilson, 1994). Geological features that give rise to lineaments include faults, shear zones, fractures, dykes, and veins as well as bedding planes and stratigraphic contacts. Geomorphic features, which appear as

lineaments on the maps, aerial photographs, and satellite images include streams, linear valleys, and ridgelines.

The intersection of lineaments is considered a good occurrence of groundwater potential zones. Lineaments like joints, fractures crisscross and faults are hydro geologically very important and may provide the pathways for groundwater movement. It may be a curve, linear, and slightly curve which is the most essential for the infiltration and movement of water to the ground (Morelli, M., and Piana, F., 2006). The weights have been given by setting more threat levels to higher lineament density which is groundwater prone. The runoff from the points of lineaments is towards the direction of the valleys cause for the productivity of groundwater recharge (Abdullahi et al.., 2013).

Geomorphology

Geomorphology was the study of the form of the earth (landforms), its description, and genesis (Gupta, 2003). In general, geomorphology reflects various landforms and structural features (Prasad, 2008). Upslope and middle slope areas are characterized by high topography and high surface runoff zones where the rate of infiltration is low or negligible with poor groundwater prospects (Rai B, 2008).

Slope factor

Topography shows the patterns of land features of the area. High slope regions have high runoff and low infiltration that are not suitable for groundwater recharge because water cannot get enough time to infiltrate the ground (Chenini et al., 2010). The flat to gentle slope area is categorized by a very high category for groundwater storage due to the nearly flat terrain, slow surface runoff allowing more time for rainwater to percolate (Prasad et al.., 2008).

Soil

Soil highly affects the movement and infiltration of ground water (Hornsby, 1986) and (Maurice and Courtney, 1990). It is the world's natural resource and a soil map is a spatial representation of these resources. A soil map is a fundamental starting point when groundwater potential zone delineation is processed.

Geology

Geology plays an important role in the distribution and occurrence of groundwater occurrence (Krishnamurthy J. A., 1995) and it plays a great role in the occurrence and delineation of groundwater potentials zone. The types of geology that are exposed to the surface are highly affected by groundwater recharge by controlling the infiltration and flow of water to the ground (Shaban, 2006).

Rainfall

Rainfall is the main source for recharging the groundwater and for all hydrological processes. From the rainfall map, the results were concluded that the annual rainfall in elevation regions is more when compared to low elevation (Rahmati, 2015). Rainfall distribution along with the slope gradient directly affects the infiltration rate of runoff water hence increases the possibility of groundwater potential zones. The zone which gives low rainfall may result in not useful for groundwater zones (Manap, 2013). Rainfall is the source of recharging groundwater (Musa, 2000).

2.7 Role of GIS and Remote Sensing in groundwater potential and recharge

According to (Mukherje, 2008) using GIS and remote sensing groundwater potential, and recharge is easily determined. For example, the different studies conducted on the Role of Satellite Sensors for the Groundwater exploration showed satellite sensors can emphasize the opened new systematic and efficient exploration of groundwater, landform mapping, geological mapping, mineral exploration, and geo-hazard studies. In addition, it helps to understand various landforms, which not easily observed. According to (Semere, 2003) Geographical information system and remote sensing is the most advanced technology for much scientific application such us monitoring natural disasters, landslide, earthquake, volcanoes, agricultural management, mineral, and groundwater exploration and can access large data at the same time which are impossible to reach such as a cliff, mountains, and gorges. (Salwa, 2015), explained the application of GIS and remote sensing and compares GIS and remote sensing applications on groundwater delineation with other methods such as geospatial, numerical modeling, and geophysical methods. He concluded that the above methods are very expensive, laborious, time-consuming, and destructive. In contrast to the above methods, according to (Tesfaye, 2012) groundwater cannot observed directly by our eyes because it is found beneath the ground many techniques give information's about groundwater and recharge potential such as hydrological

investigation, geophysical and geo-electrical or geophysical seismic refraction methods which are very expensive and time-consuming.

GIS and remote sensing are the latest, time, and cost-effective technology for groundwater exploration by acquiring full information and access to all parameters of factors that control groundwater potentials and recharge areas by using different software easily. The different works are done on groundwater potential and recharge determination by using GIS and remote sensing. From those, (Chowdhury et al., 2009) conducted on integrated remote sensing and GIS-based for assessing groundwater potential in west Medinipur district, India and they Defined when GIS and remote sensing techniques have increased for using groundwater potential and recharge zone mapping.

2.8 Hydrological models

Hydrological models are simplified systems to compute the processes of the hydrological cycle (Precipitation, Infiltration, Interception, Evaporation, and Runoff). In an entire river basin, based on a set of interrelated equations that try to convert the physical laws, which governs the complex natural phenomena (Barbara, 2008).

Based on the description of physical process, the hydrological models can be classified into three groups like conceptual models, physically based distributed models and empirical models (Beven, 2001). Physically based distributed models (sometimes called white-box models) presumably are the consequences of the most important laws governing the phenomena. The model has a logical structure similar to the real-world system and may be helpful under changed circumstances. It is designed by the principles of physical processes based on continuity and the conservation of mass, energy and momentum. These model used a number of model parameters represents the different heterogeneities in the catchment. e.g. infiltration model, evaporation model, SHE models. In the recent time, advances have been made in hydrological process understanding and modeling using topography driven, conceptual, flexible, semi-distributed model structures (Gharari et al., 2013).

The regional groundwater models used for identifying and analyzing groundwater system (infiltration-percolation-discharge relations) are often quasi-steady state and therefore it needs a long-term average input data. Thus, WetSpass, which yields spatially varying groundwater recharge using spatially varying soil, land-use, and meteorological inputs, can be used for

understanding the characteristics of groundwater recharge (Batelaan and Woldeamlak, 2003). Empirical models (Black box) which mathematical correlations are obtained based on the observed data analysis rather than based on the physical processes in the catchment e.g. Unit hydrograph-based model, Linear regression model. Conceptual models (sometimes called grey-box models) are intermediate between theoretical and empirical models which were consider physical laws in highly simplified form (Dandy & Maier, 2005)

2.9 The WetSpass Model

The WetSpass model was built as a physically distributed based methodology for estimation of the long-term average, spatiotemporally varying, water balance components like groundwater recharge, surface runoff, and actual evapotranspiration. It is an acronym for water and energy transfer between soil, plants and atmosphere under quasi-steady state that was built upon the foundations of the time dependent spatially distributed water balance model (Batelaan & DeSmedt, 2001). The model estimates seasonal and annual long-term spatial distribution amounts of groundwater recharge by subtracting the seasonal and annual surface runoff and evapotranspiration from the seasonal and annual precipitation respectively (Arefaine et al., 2012). The WetSpass was successfully applied in Belgium (Batelaan and De Smedt, 2001), Geba watershed, Ethiopia (Tesfamichael, et al., 2010) and in Werii watershed in Ethiopia. Based on those authors, the finding in Melkaoda watershed for groundwater recharge was successfully simulated which was the main interest of this research. In Ethiopia, several authors were used WetSpass model for their groundwater recharge estimation studies.

2.10 Analytical Hierarchy Process Methods

The Analytic Hierarchy Process (AHP) is a general theory of measurement. It is used to derive ratio scales from both discrete and continuous paired comparisons. These comparisons may be taken from actual measurements or from a fundamental scale that reflects the relative strength of preferences and feelings. The AHP has a special concern with departure from consistency, its measurement, and dependence within and between the groups of elements of its structure. It has found its widest applications in multi-criteria decision making, planning, and resource allocation and in conflict resolution (Saaty, 1980: Saaty and Vargas, 1981: Saaty, 1982)

Different researchers use different weight overlay and decision-making analysis methods. from those researchers (Sajikumar and Gigo, 2013) adopt thematic layers of soil, slope, geology,

Landuse/land cover, lineaments, and drainage gave accurate information about groundwater occurrence and generate the result from Weight Index Overlay Analysis (WIOA) by employing analytical hierarchy process methods. Finally, conclude that the analytical hierarchy process is a promising method for groundwater exploration.

The rates for the classes in a layer and weights for the thematic layers were computed based on saaty's AHP (Saaty, 1980)). Saaty's AHP is the most widely accepted method for scaling the rates/weights of factors whose entries indicate the strength with which one factor dominates over the other about the relative criteria (Tesfaye, 2010). In this method, the relative importance of individual class within the same map and thematic maps were compared to each other by pairwise comparison matrices. As such, matrices were constructed, where each criterion was compared with the other criteria, relative to its importance, on saaty's scale from 1 to 9. A score of 1 represents equal importance between the two factors, and a score of 9 indicates the extreme importance of one factor compared to the other one as shown in table 2.5 below.

3. MATERIAL AND METHODS

3.1 Description of the study area

3.1.1 Location and area

Melkaoda Watershed, where this study was conducted is located in Oromia Regional State, Rift Valley Lakes Basin, Southern Ethiopia (Figure 3.1). The watershed touches three administrative districts: Kofele, Shashemene, and Aje. The area covered by the watershed is 315 km^2. Astronomically, the study area extends from 7º 11'45''N to 7º 23'N latitude and 38º 30'81''E to 38º46'71''E longitude. In relative terms, the study area is located at a distance of 250km along with Addis Ababa- Shashemene road.

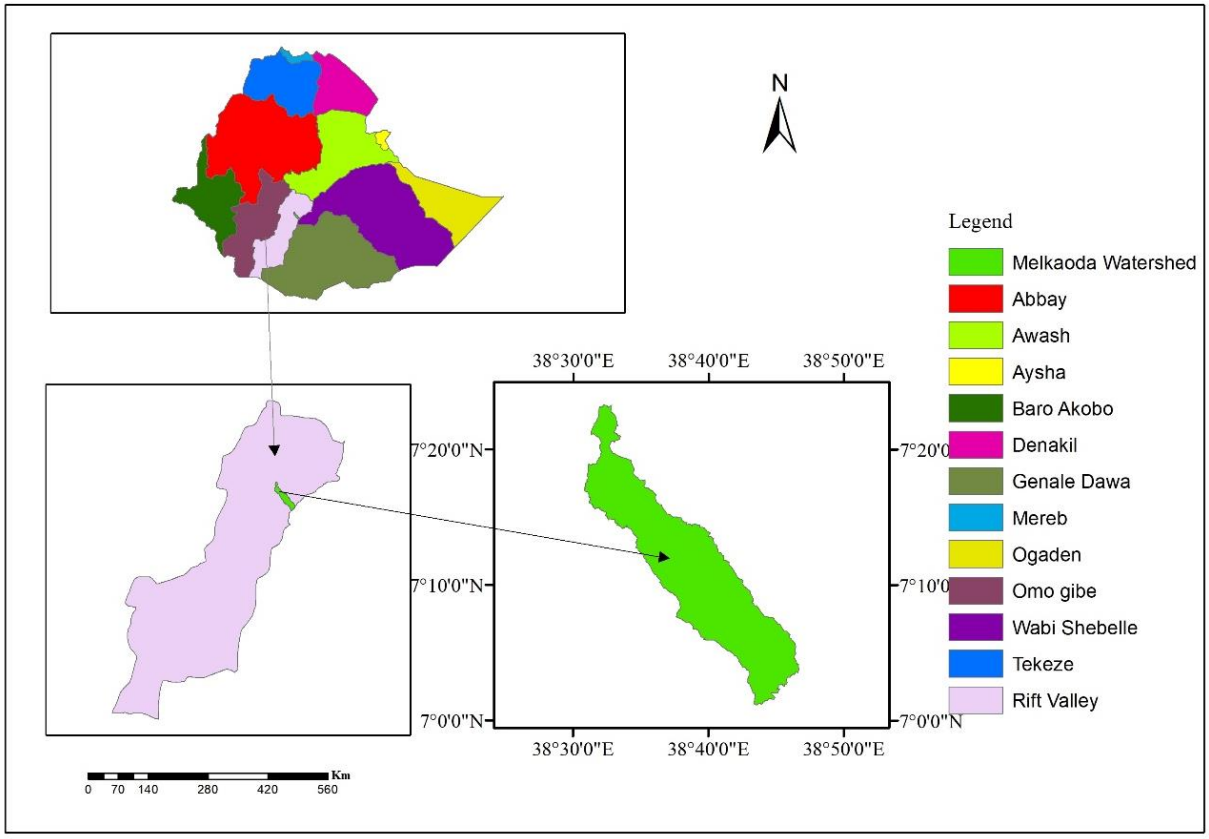

Figure 3. 1: Study area location

3.1.2 Topography

Under a regional topography, the area is one part of the Easter escapement of Main Ethiopia Rift (MER which is mostly characterized by plain within some undulating land features. Particularly the study area is bounded by gently sloping land feature from the eastern part which

is gently declining towards Lake Shalla. The average elevation in theWatershed is 2193.67m above mean sea level. The peak altitude of the area is 2687m around Kofele ridges and the lowest is 1749m to the flat area of the study area. The slope is also another topographical aspect that influences the delineated groundwater potential and the slope of the study area ranges from 0 to 34.78^{o}.

3.1.4 Climate

The average altitude of the study area is 2193.67m which is between the altitude intervals of 1749-2867m. This altitude infers that the area has a 13.45-17.27c^{0} mean annual temperature which classifies the area under the sub-tropical zone. Temperature is the major meteorological factor that was affecting evapotranspiration, surface runoff and groundwater recharges. The higher the air temperature, the more vapor it can hold, and similarly if the temperature of evaporating water is high, it can more readily vaporize (Shaw, 1994). The study area falls under a bi-modal rainfall pattern. That means the study area gets rainfalls during March-June and August-September without distinct dry periods separating the two wet seasons. The study area has a high infiltration rate and some surface runoff which interconnected to porous of the geologic formation of the area.

3.2 Data collection and Analyses

3.2.1 GIS and RS-based Groundwater Potential Zone Identification

To meet this objective, rainfall, geomorphology, geology, drainage density, soil, slope, landuse, and lineament density data were used to develop thematic layers and for further analyses using Saaty's AHP method (Annesh and Paresh, 2015). The above-listed thematic layers were considered in this study as they were widely used in similar studies in various parts of the world (Waikar and Aditya, 2015: Zeinolabedinia and Esmaeily, 2015:Tesfa and Girum, 2019). The following sub-sections are provided as to how these thematic layers were developed and how the AHP method was applied to develop groundwater potential maps for the study area.

3.2.1.1 Rainfall data

Annual rainfall data of three meteorological stations, which are found in and around the study area (Kofele, Shashemene, and kuyera) were collected from the Ethiopia National Meteorology

Agency. The data are presented in Appendix 7.3. The collected data were checked for continuity, homogeneity, and consistency as described below.

Continuity check and estimation of missed data

Missing rainfall data can be estimated by either the arithmetic mean method or the normal ratio method. If the normal (long term mean) annual rainfall at each index station is within 10% of that for the station with the missing record, simple arithmetic mean of rainfall at index stations will provide an approximate value for the missing record, otherwise normal ratio method is applied (Subramanya, 2008). In this study, the normal ration method was used as the variation in the mean annual rainfall values were found to be more than 10%.

The equation of the Normal Ratio Method is given below

$$P_A = \frac{1}{n}\left(\frac{N_A P_B}{N_B} + \frac{N_A P_C}{N_C} + \cdots + \frac{N_A P_N}{N_N}\right) \qquad Eq.3.1$$

where, N_A, N_B, N_C…N_N=normal annual rainfall values at station A, B, C …N: P_B, P_C… P_N =rainfall records at index stations at the time of missing records and P_A= an estimated value for missing record at station A.

Homogeneity test

Homogeneity analyses are used to identify a change in the statistical properties of the time series. The causes can be either natural or man-made. These include alterations to landuse and relocation of the observation station. Therefore, to select the representative meteorological station for the analysis of areal rainfall estimation, checking the homogeneity of group stations is essential and the homogeneity of the selected gauging station's monthly rainfall records was carried out by non-dimensional parametrization.

$$Pi = \frac{Over\ year\ average\ monthly\ PCP\ for\ month\ i}{the\ over\ years\ average\ yearly\ PCP\ of\ station} \qquad Eq.3.2$$

where Pi: non-dimensional values of precipitation for a month i, PCP: precipitation of the station

The selected stations were also plotted for comparison with each other in Figure 3-2. They showed the same model and pattern for the selected station. These assure that the selected stations were homogenous.

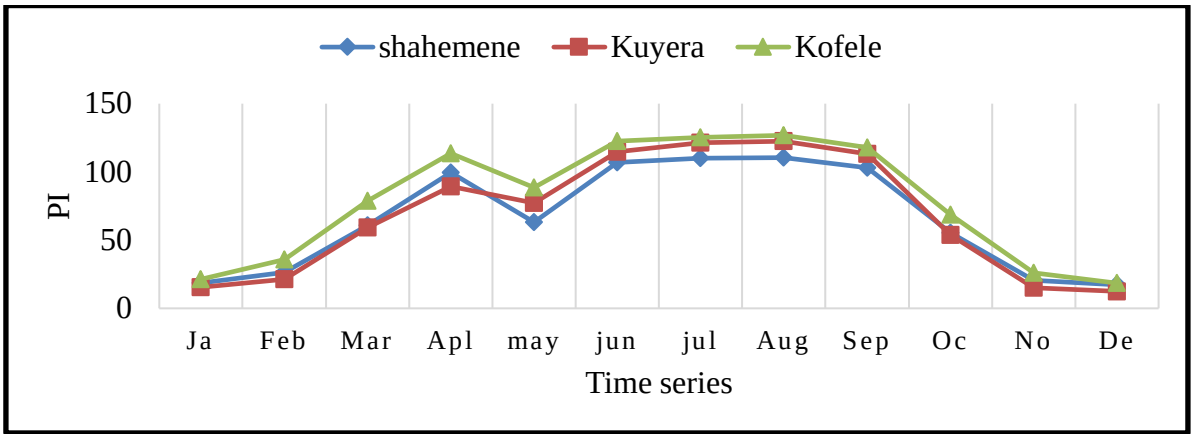

Figure 3. 2: Homogeneity test for the stations used

Consistency test

A double mass curve (DMC) was used to check the consistency of rainfall for adjustment of inconsistent data. This technique is based on the principle that when each recorded data comes from the same parent sample, they are consistent. A double-mass curve is a graph of the cumulative catch at the rain gauge of interest versus the cumulative catch of one or more gauges in the region that has been subjected to similar hydro-meteorological occurrences and is known to be consistent. The double-mass curve will have a constant slope if a rainfall record of the hydro-meteorological occurrences for the record is consistent. A change in the slope of the double mass curve would suggest that an external factor has caused changes in the character of the measured values. If a change in slope is evident, then either the record needs to be adjusted with either the early or the later period of record which is not disturbed.

$$Pcx = Px * \left(\frac{Mc}{Ma}\right) \quad \text{(3.3)}$$

Where: Pcx = corrected precipitation at any time t_1 at station X; Px = originally recorded precipitation at time t_1 at station X; Mc = corrected slope of the double-mass curve; Ma = original slope of the double-mass curve.

Development of areal rainfall data

In applying meteorological to the catchment of a few square kilometers for the estimation of groundwater potential zone, it is often necessary to estimate the average areal rainfall for a catchment from rain gauge observation. For this task inverse distance weight (IDW) interpolation techniques were applied in ArcGIS. In the IDW interpolation method, the sample points are weighted during interpolation such that the influence of one point relative to another

decline with distance from the unknown point to be created weighting is assigned to sample points through the use of a weighting coefficient that controls how the weighting influence will drop off as the distance from new point increases. The greater the weighting coefficient, the less the effect points will have if they are far from the unknown point during the interpolation process.

Then, the map is assigned and converted to a characteristic spatial representation format to make them suitable for analyses in GIS environments.

The Mean Annual rainfall data is calculated from the rain gauge station for the past 30 years.

Rainfall distribution along with the slope gradient directly affects the infiltration rate of runoff water hence increases the possibility of groundwater potential zones.

The prepared rainfall map is classified into five categories depending on their relation with groundwater potential zone prospects as shown in (Figure 3.3) below. These were (1096.85-1214.08mm) very high groundwater potential zone, (977.72-10196.85) high groundwater potential zone, (862.38-977.72mm), moderate groundwater potential zone, (784.86-862.38mm) low groundwater potential zone, and (731.91-784.86mm) very low groundwater potential zone. The major area of the study area was dominated by the normal rainfall quantity of 784.86-862.38mm.

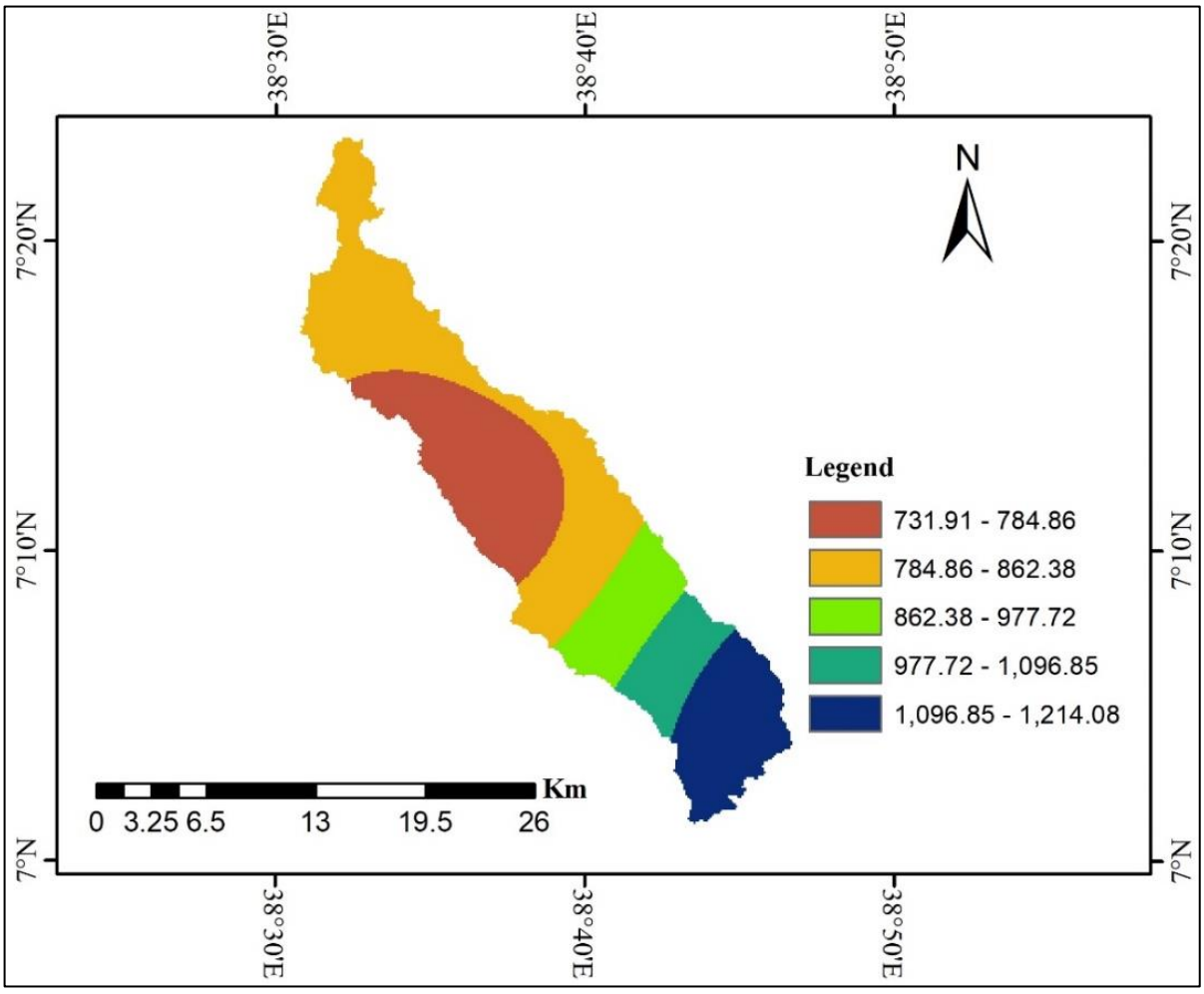

Figure 3. 3: Rainfall map of the study area

Once the collected rainfall data was processed in the required manner, a rainfall thematic layer was developed with classes for appropriate groundwater potential mapping. The following table is depicted to give these classes. The classes were developed as per the recommendation by (Tolche, 2021; Zeinolabedinia, and Esmaeily, 2015) more Precipitation, higher weight.

Table 3. 1: Annual rainfall classification for groundwater potential zoning

Annual rainfall (mm)	Classes for groundwater potential zoning	Remarks
1096.85-1214.08	Very high	5
977.72-1096.85	High	4
862.38-977.72	moderate	3
784.86-862.38	low	2
731.91-784.86	Very low	1

3.2.1.2 Landuse/Landcover map

To develop the landuse/land cover map of the study area, a satellite image of the study area for the year 2018, and Landsat 8 OLI images were downloaded from the USGS website. The downloaded satellite image was processed using ERDAS imagine by carrying out the process like layer stacking, sub-setting the study area from a stacked image, and then was classified using the supervised classification technique. After preprocessing finished, image classification was done. The final stage, image post-classification was then carried out. Accuracy assessment of the classified images was done for verification and validation of the results as described below.

Accuracy assessment

Accuracy assessment is an important step in the image classification process. It is a process used to estimate the accuracy of image classification by comparing the classified map with a reference map (Caetano et al., 2005). Error matrix was used to derive a series of descriptive and analytical statistics for accuracy assessment (Manandhar et al., 2009). The columns of the matrix depict the number of pixels per class for the reference data, and the rows show the number of pixels per class for the classified image. From this error matrix, overall accuracy, user's and producer's accuracy were reported. Based on Google Earth Map, which was not used for

classification purposes, the confusion matrix table was produced in Table 3.2. This matrix compares the relation between known reference data (ground truth) and the corresponding results of the classification.

Table 3. 2: Confusion Matrix Table for 2018 landuse and land cover

	Reference Data					
Classified Data	Bare Land	Agricultural Land	Built-up Area	Forest area	Grassland	Total User
Bare Land	58	5	6	2	2	73
Agricultural Land	2	120	2	4	1	129
Built up Area	3	6	70	0	1	80
Forest area	1	7	6	62	3	79
Grassland	1	2	6	2	73	84
Total Producer	65	140	90	70	80	445
Number of LULC correctly classified=383 Overall Classification Accuracy% = ((58+120+70+62+73)/(445))*100 = 86.07%						

As shown in Table 3.2 above, the confusion matrix indicates that the overall accuracy assessment is very strong i.e. 86.07% which is greater than the requirement for strongly acceptable classification, i.e. 84% (Anderson, 1997). The users and producer's accuracy assessment also calculated for each land class and indicated acceptable agreement. The kappa hat value of 0.854 indicates a better accuracy that the classification has resulted from random sample class classification. Since the kappa hat value fell above 80%, it represents strong agreement. User accuracy: User accuracy is a measure indicating the probability that a pixel is a Class of the sample given that the classifier has labeled the pixel into sample class as shown in Table 3.3.

Table 3. 3: Users and producers accuracy table

Class Name	Users Accuracy	Producers Accuracy
Bare Land	58/73*100 =79.45%	58/65*100 =89.23%
Agricultural Land	120/129*100 =93.02%	120/140*100 =85.71%
Built up Area	70/80*100 =87.5%	70/90*100 =77.78%
Forest area	62/79*100 =78.48%	62/70*100 =88.57%
Grassland	73/84*100 =86.91%	73/80*100 =91.25%

Producer accuracy: Producer accuracy is a measure indicating the probability that the classifier has labeled an image pixel into the sample area given that the ground truth of the sample area.

Overall Accuracy: The overall accuracy is calculated by summing the number of pixels classified correctly and dividing by the total number of pixels sampled. The ground truth image or ground truth training area defines the true class of the pixels. The pixels classified correctly are found along the diagonal of the confusion matrix table which lists the number of pixels that were classified into the correct ground truth class. The total number of pixels is the sum of all the pixels in all the ground truth classes. The kappa coefficient is calculated by multiplying the total number of pixels in all the ground truth classes by the sum of the confusion matrix diagonals, subtracting the sum of the ground truth pixels in a class times the sum of the classified pixels in that class summed over all classes, and dividing by the total number of pixels squared minus the sum of the ground truth pixels in that class times the sum of the classified pixels in that class summed over all classes as shown in table 3.4. In addition, it is a way to measure the actual agreement and chance agreement between the reference data and the classified data. The Kappa coefficient represents the proportion of agreement obtained after removing the proportion of agreement that could be expected to occur by chance (Foody, 2002). This would be expressed in terms of the percentage of strong, moderate and poor agreement i.e. a value >0.80 (80%) strong agreement; a value b/n 0.40 and 0.80 (40 to 80%) represents moderate agreement; and a value < 0.40 (40%) represents poor agreement.

Table 3. 4: Conditional kappa coefficient for each LULC

Landuse land cover types	Conditional kappa for each LULC class	Kappa coefficient in Percent (%)
Bare Land	$\frac{(383 * 445) - (65 * 73)}{(445 * 445) - (65 * 73)} = 0.857$	85.7
Agricultural Land	$\frac{(383 * 445) - (140 * 129)}{(445 * 445) - (140 * 129)} = 0.847$	84.7
Built-up Area	$\frac{(383 * 445) - (90 * 80)}{(445 * 445) - (90 * 80)} = 0.855$	85.5
Forest area	$\frac{(383 * 445) - (70 * 79)}{(445 * 445) - (70 * 79)} = 0.856$	85.6
Grassland	$\frac{(383 * 445) - (80 * 84)}{(445 * 445) - (80 * 84)} = 0.855$	85.5
Overall kappa statistics =0.854		85.4

After passing through long processes, the landuse/land cover of the study area was classified into five classes as grassland, forest land, buildup land, bare land, and agricultural land as shown in Figure 3.4 below. Out of 315km^2 of the study area 161.18, 11, 46.02, 27.21, and 69.6 km^2 felt under agriculture, bare land, forest land, grassland, and buildup respectively with an overall accuracy percent of 86.07 and kappa hat coefficient of 0.854 which has a great agreement with (Anderson, 1997) values.

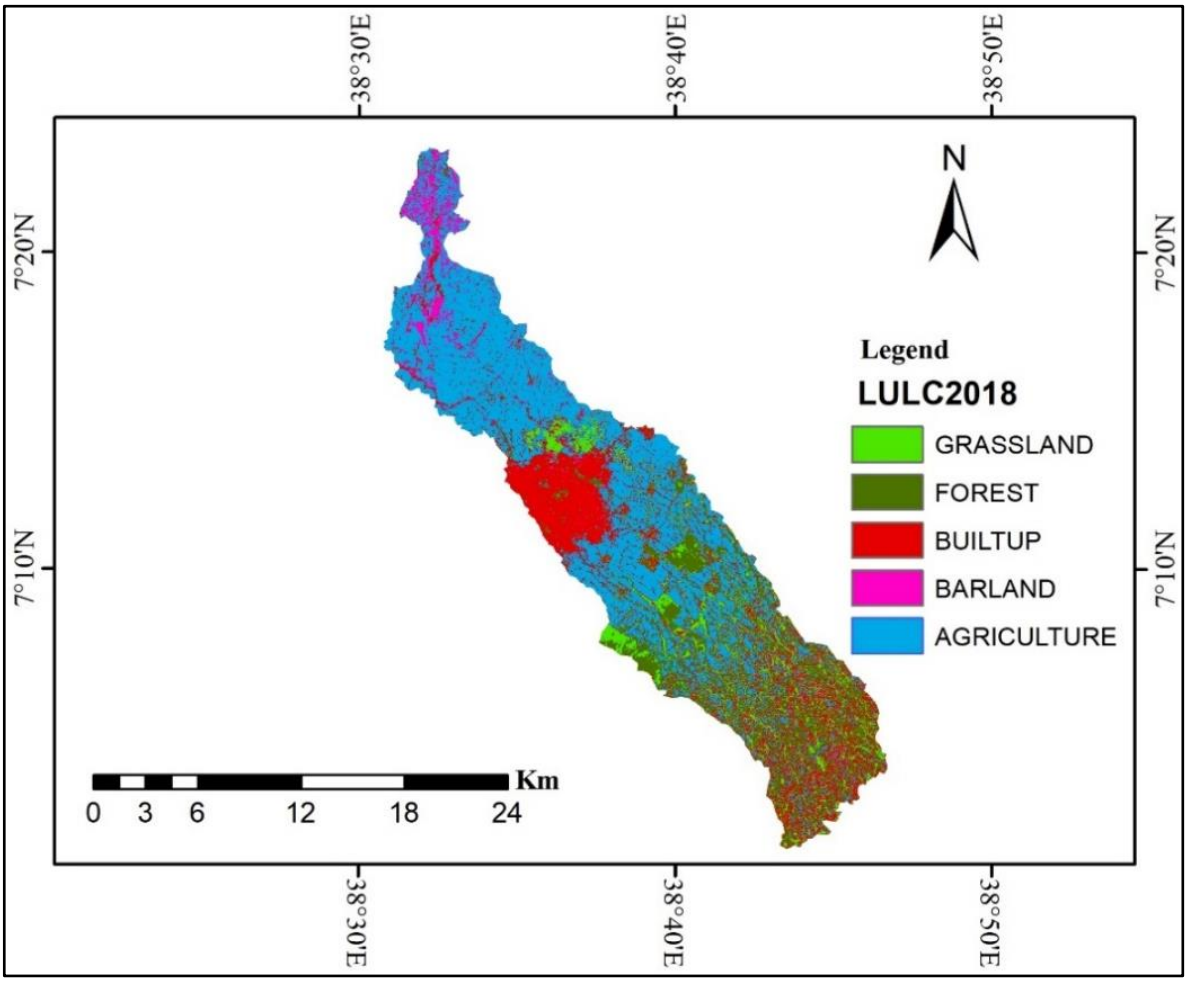

Figure 3. 4: Landuse/Land cover map of the study area

Once the classified landuse/land cover map was checked for accuracy and processed in the required manner, a landuse/land cover thematic layer was developed with classes for appropriate groundwater potential mapping. The following table was presented to show these classes. The classes were developed as the recommended (Tolche, 2021; Andualem, and Demeke,2019).

Table 3. 5: Landuse classification for groundwater potential zoning

Landuse classes	Classes for groundwater potential zoning	Remarks
Forest area	Very high	5
Agricultural Land	high	4
Grassland	Moderate	3
Bare Land	Low	2
Built up Area	Very low	1

3.2.1.3 Drainage density

To develop the drainage density map of the study area, a digital elevation model (DEM) of the study area was downloaded from the USGS website. The downloaded DEM was processed using ArcGIS environment by applying line density method that included different processes like filling sinks, creating flow direction, creating flow accumulation, creating stream order, and finally converted stream order to features then drainage density map was obtained.

Drainage density of the study area was classified into five categories which were 0.0-1.87 km/km^2, 1.87-2.92 km/km^2, 2.92-4.27 km/km^2, 4.27-5.35 Km/Km2 and 5.35-6.89 km/km^2 as shown in figure 3.5 below.

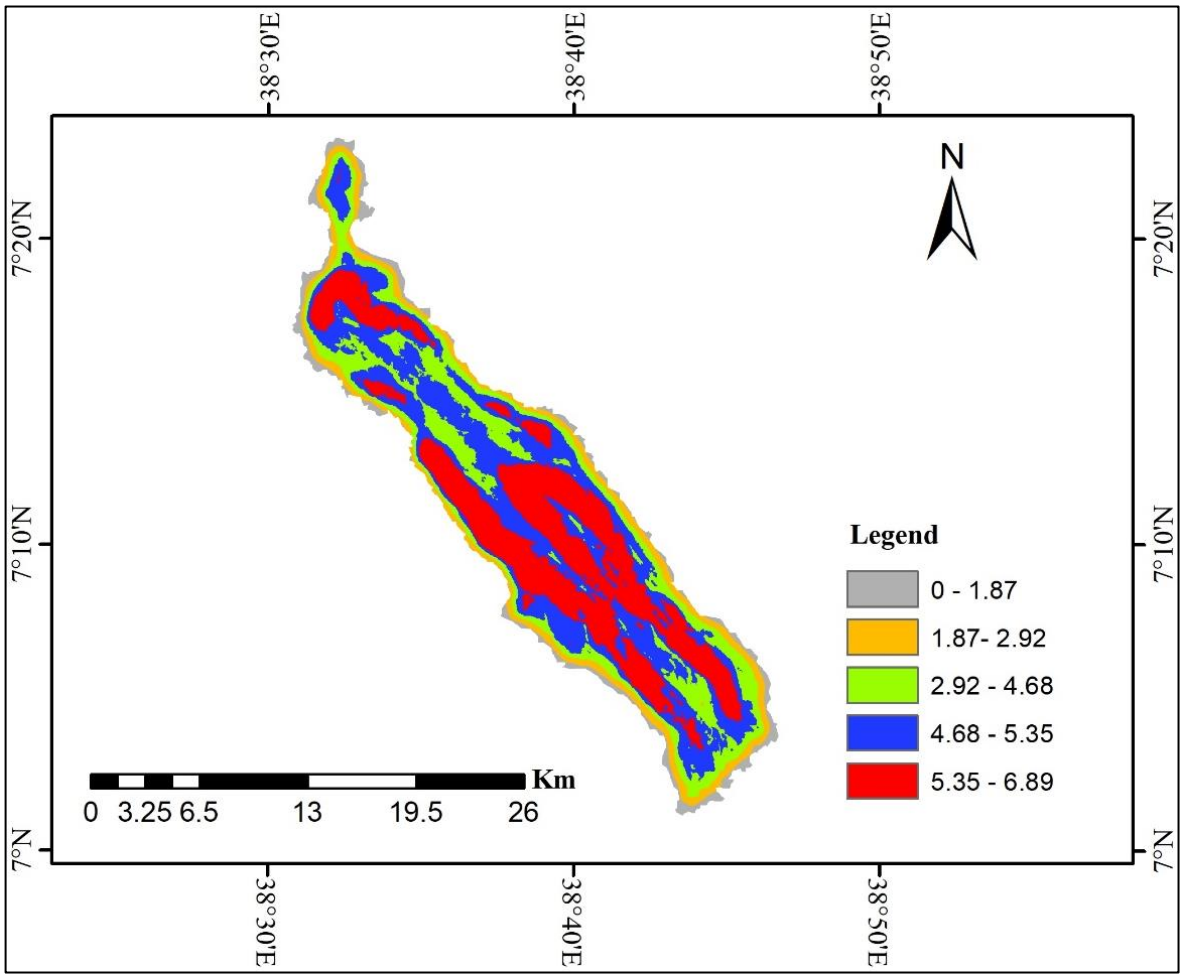

Figure 3. 5: Drainage density map of the study area

Once the obtained map was prepared in the required manner, a drainage density thematic layer was developed with classes for appropriate groundwater potential mapping. The following table is depicted to give these classes. The classes were developed as per the recommendation by (Tolche, 2021; Waikar, and Nilawar, 2014).

Table 3. 6: Drainage density classification for groundwater potential zoning

Drainage density	Classes for groundwater potential zoning	remarks
0-1.87	Very high	5
1.87-2.92	High	4
2.92-4.68	moderate	3
4.68-5.35	low	2
5.35-6.89	Very low	1

3.2.1.4 Lineament density

To develop the lineament density map of the study area, satellite image of the study area for the year 2018, Landsat 8 OLI images were downloaded from the USGS website which used for landuse map preparation was used again to obtain this map. The downloaded satellite image was processed using PC Geomatics software then the line density method was used in the ArcGIS environment.

The lineament density was classified into five types of lineament density quantified as 0-0.34, 0.35-0.87, 0.87-2.66, 2.66-3.55, and 3.55-4.45.major area of the land was cover by lineament density of 0-0.34km/km^2 and less area of the study area was dominated by 3.55-4.45km/km^2 (Waikar and Nilawar, 2014), classified lineaments into two types based on their length. Minor lineaments- For quantification purposes, lineament with length < 3 km is classified as a minor lineament. Major lineaments- Lineament with length > 3 km is classified as a major lineament. This study area was covered by minor lineament and major lineament, magnitude varies from 0-4.45 Km/km^2.

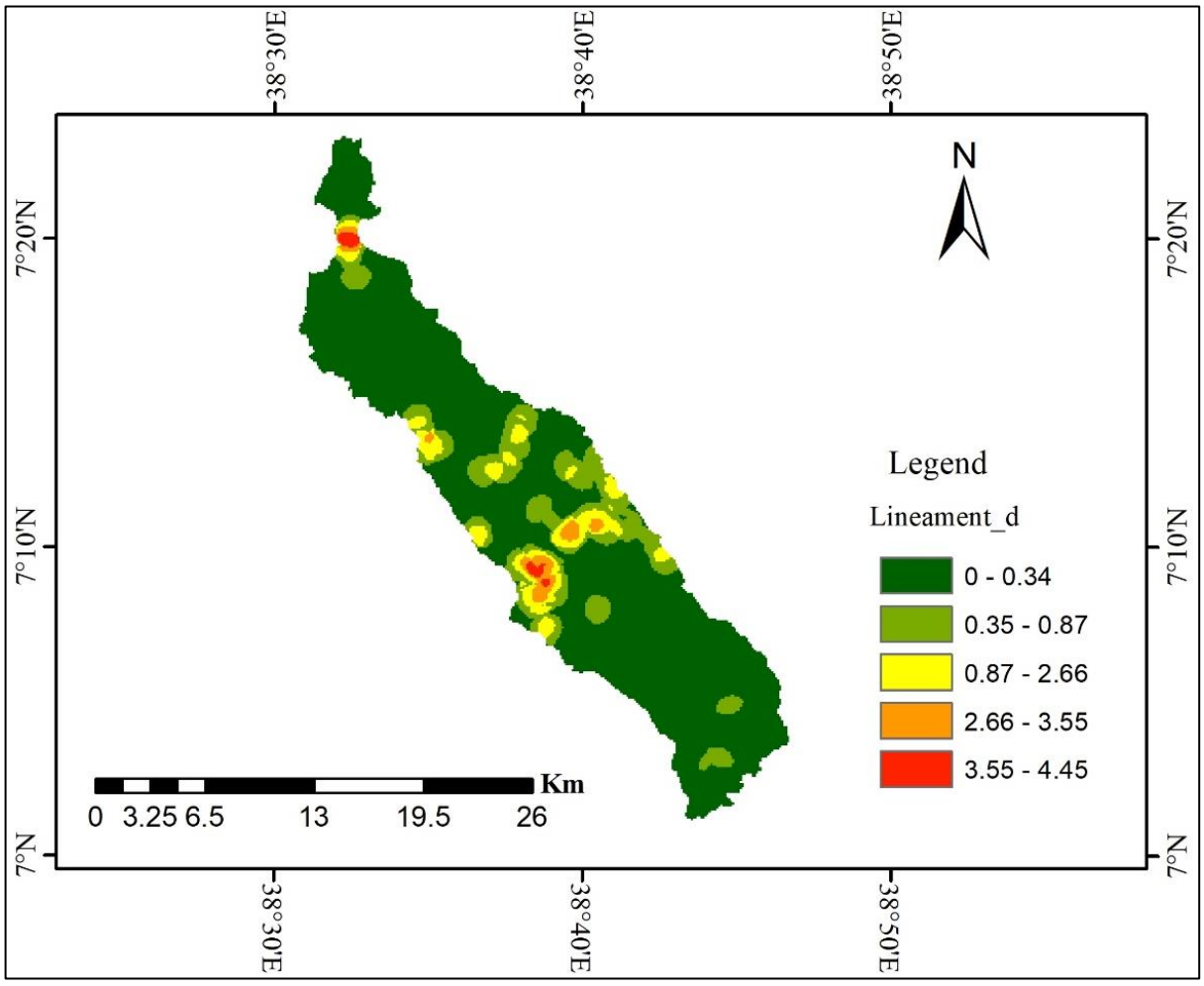

Figure 3. 6: Lineament density map of the study area

Once the generated map was prepared in the required manner, a Lineament density thematic layer was developed with classes for appropriate groundwater potential mapping. The following table is depicted to give these classes. The classes were developed as per the recommendation by (Waikar and Nilawar, 2014; Tolche, 2021).

Table 3. 7: Lineament density classification for groundwater potential zoning

Lineament density	Classes for groundwater potential zoning	Remarks
0-0.34	Very low	1
0.34-0.87	low	2
0.87-2.66	moderate	3
2.66-3.55	high	4
3.55-4.45	Very high	5

3.1.2.5 Geomorphology

To generate the geomorphology map of the study area, the DEM of the study area was downloaded from the USGS website. The downloaded DEM was processed using SAGA GIS software then terrain analysis following terrain classification and TPI (topographic position index)-based landform classification method was used and finally it was processed in ArcGIS environment for further analyses.

The geomorphological features of the area are classified into five features to know about the water resources in the area as drainage, plains, valleys, upslope and middle slope as shown in Figure 3.7 below. In the study area, the major land of the area was dominated by plains that might affect the potential of the groundwater in a great amount. Then, the map is assigned and converted to a characteristic spatial representation format to make them suitable for analysis in GIS environments.

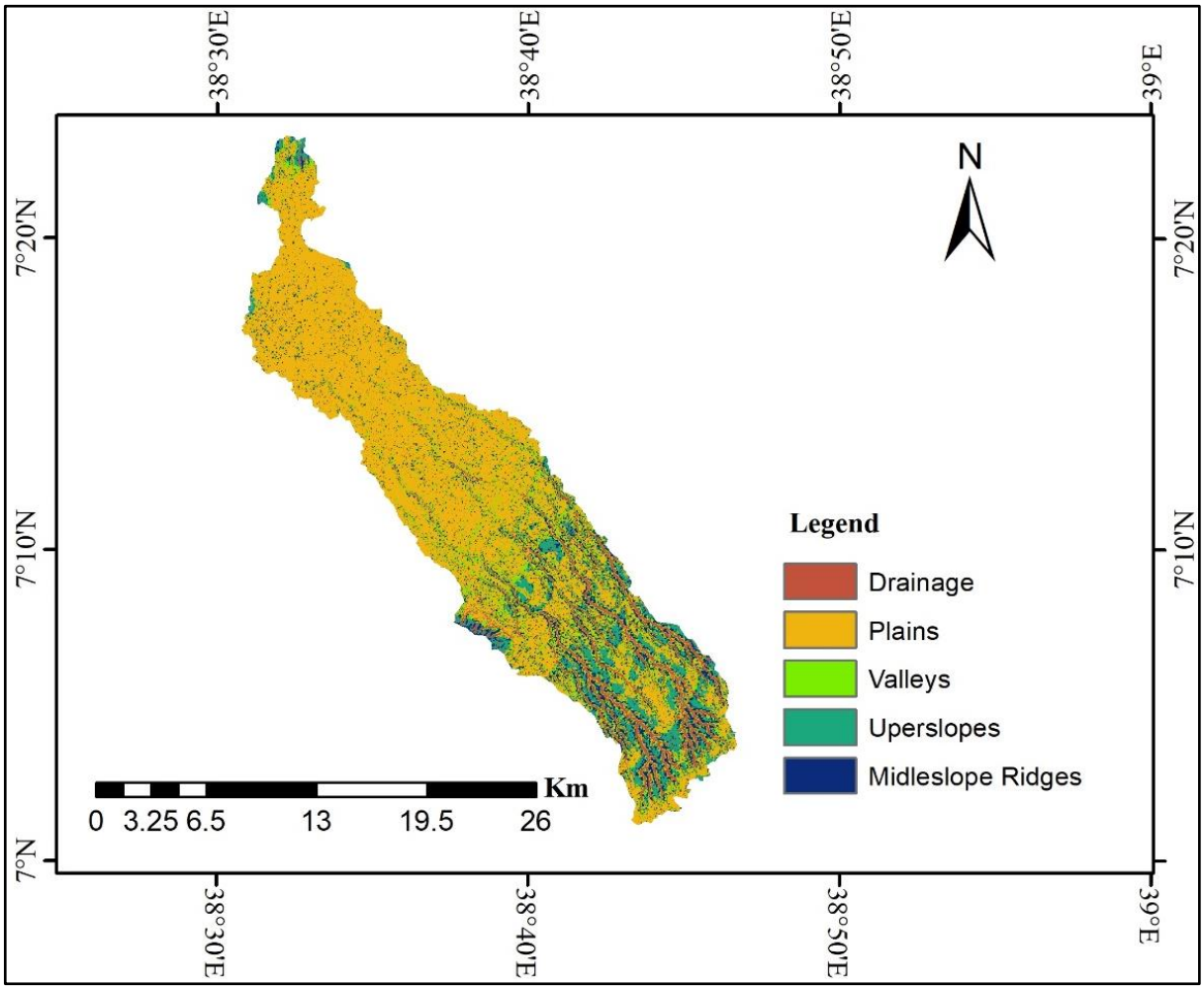

Figure 3. 7: Geomorphological map of the study area

Once the developed map was prepared in the required manner, a geomorphology thematic layer was developed with classes for appropriate groundwater potential mapping. The following table is depicted to give these classes. The classes were developed as per the recommendation by (On, 1768; Arnot & Grant, 1981) description of landform classification.

Table 3. 8: Geomorphology classification for groundwater potential zoning

Landform elements	Slope level	Classes for groundwater potential zoning	remarks
plain	Flat area	Very high	5
valley	Low slope	high	4
Middle slope ridge	Moderate slope	moderate	3
Upper slope	Moderate to strong slope	Low	2
Drainage	Moderate to strong slope	Very low	1

3.1.2.6 Slope factor

To generate the slope map of the study area, the DEM of the study area was downloaded from the USGS website. The downloaded DEM was processed using ArcGIS then slope (spatial analyses tools) was used and finally it was processed in the ArcGIS environment for further analyses. The identified slope of the study area category varies from (0-34.99^{o}) and the area was classified into five classes like (0-2.882^{o}) flat, (2.882-5.9^{o}) gently sloping, (5.900-10.292^{o}) moderately sloping, (10.292-16.19^{o}) steeply sloping, and (16.19-34.99^{o}) strongly steeply sloping. Flat slope (0-2.882^{o}) indicates the presence of very high groundwater potential zones where a steep slope (16.19-34.99$^{o)}$ shows the presence of very low groundwater potential zones as water runs rapidly off the surface and does not have sufficient time to infiltrate the surface, keeping other parameters constant. The major area of the study area was dominated by flat areas which might affect groundwater at a great rate.

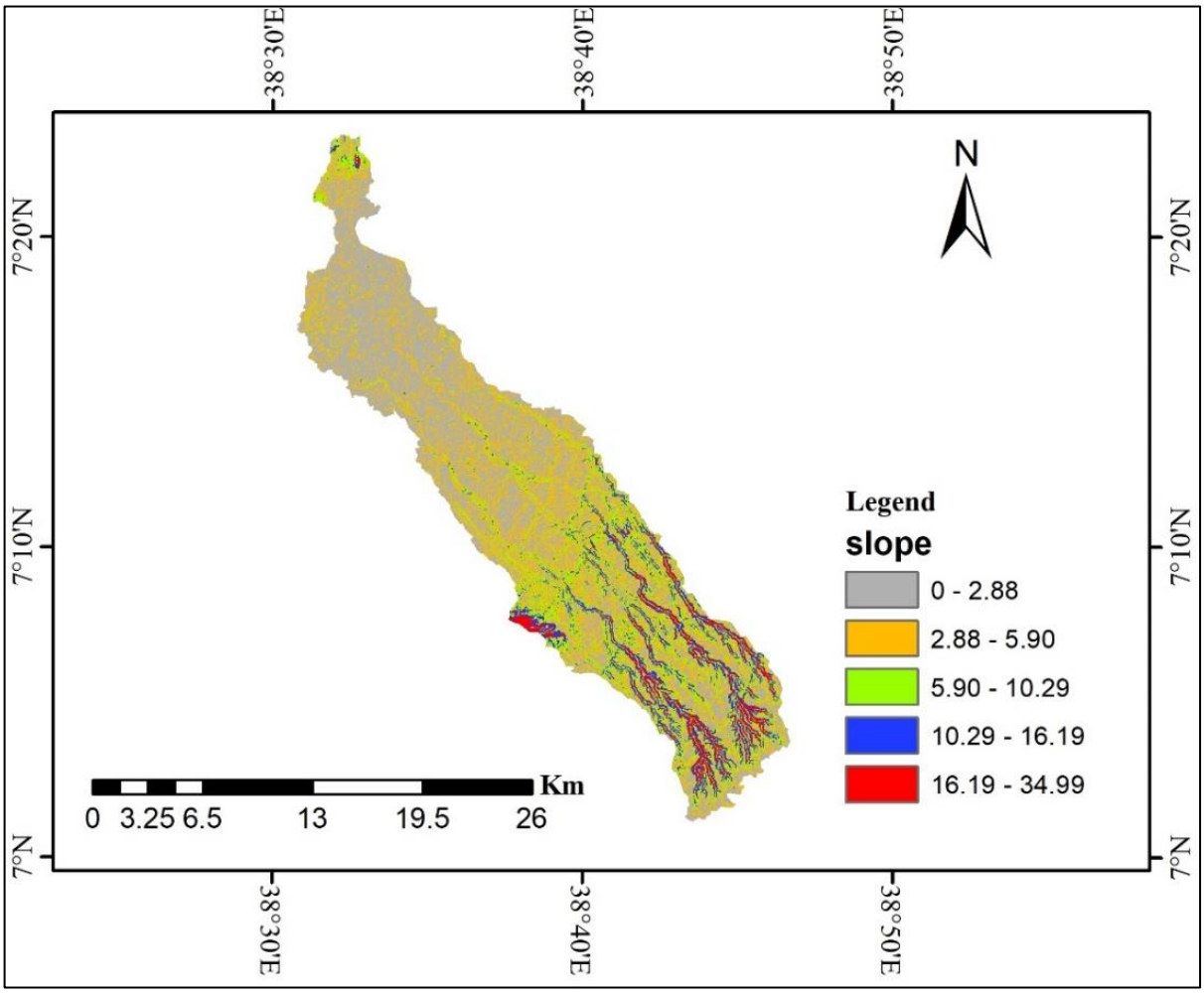

Figure 3. 8: Slope map of the study area

Once the developed map was prepared in the required manner, a slope thematic layer was developed with classes for appropriate groundwater potential mapping. The following table was presented to give these classes. The classes were developed as per the recommendation by (Daniel et al.., 2018; Waikar and Nilawar, 2014) have reported Slope gradient and category.

Table 3. 9: Slope classification for groundwater potential zoning

Slope in degree	Classes for groundwater potential zoning	remarks
0-2.882	Very high	5
2.882-5.9	high	4
5.9-10.292	Moderate	3
10.292-16.19	low	2
16.19-34.99	Very low	1

3.1.2.7 Soil

To develop the soil map of the study area, the soil data for this task was collected from the ministry of water, energy and irrigation and the map was prepared by clipping from the obtained soil data in the GIS environment. Soils of the study area are classified into four textural classes based on their grain size using the United States Department of Agriculture (USDA) textural classification methods, sandy loam, clay, sandy clay loam, and loam.

In the study area, there are four major types of soil which are stated below. These include the soil's textural classes like clay soil, sandy clay loam, loam, and sandy loam. All these soil textural classes influence the groundwater infiltration and alter the rate of percolation of precipitation. Next to sandy clay loam, clay, and loam soil were the major soil covered in the study area as shown in figure 3.9 below.

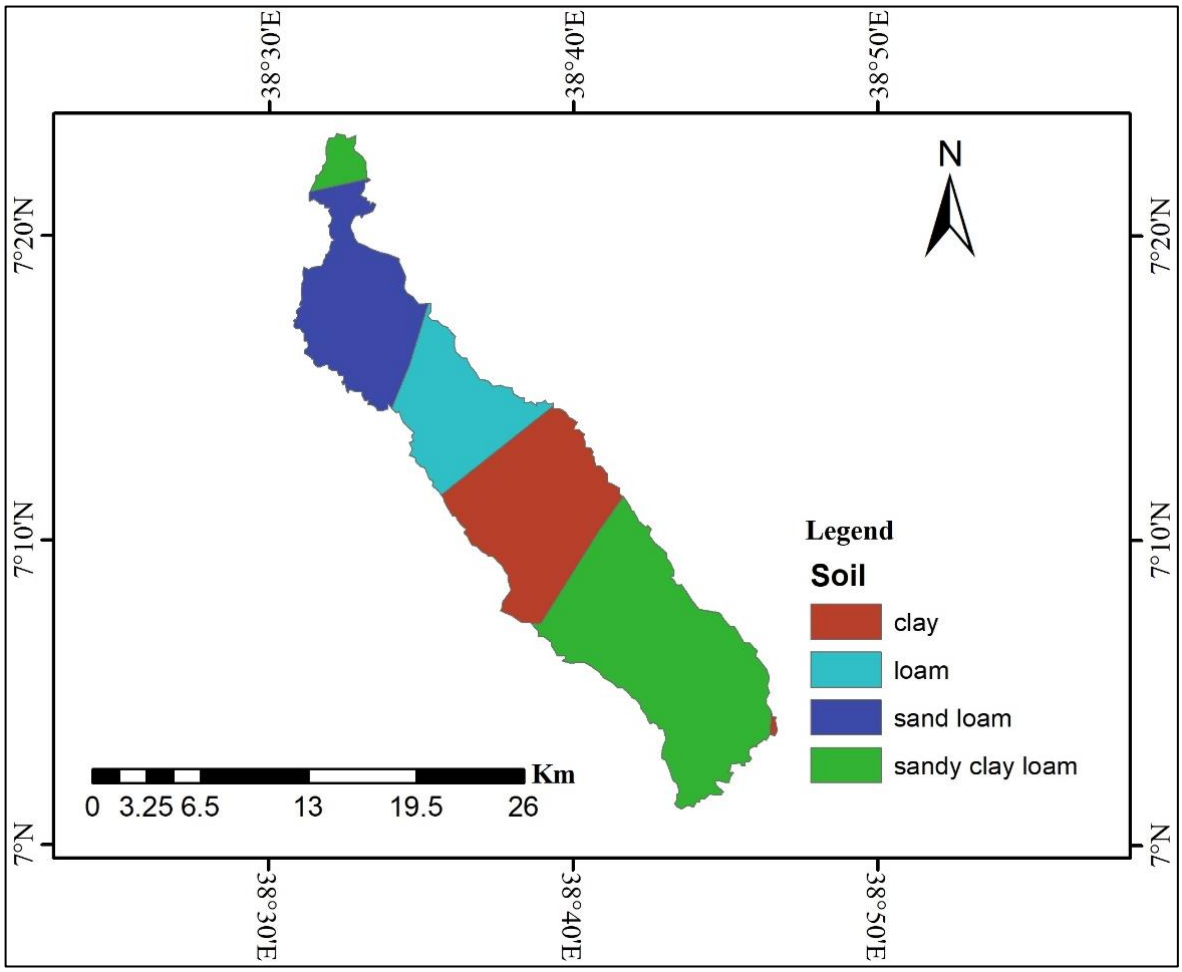

Figure 3. 9: Soil map of the study area

Once the developed map was prepared in the required manner, a soil thematic layer was developed with classes for appropriate groundwater potential mapping as recommended by (Tolche, 2021). The following table was presented to show these classes.

Table 3. 10: Slope classification for groundwater potential zoning

Soil textural classes	Classes for groundwater potential zoning	remarks
Sandy loam	Very high	5
Loam	High	4
Sandy clay loam	Moderate	3
Sandy clay loam	Moderate	3
Clay	Low	1

3.1.2.8 Geology

To develop the geology map of the study area, the geology data for this task was collected from the Geological Survey of Ethiopia and the map was prepared from this data by clipping method in the GIS environment. The geology of the study area was classified into five classes based on their capability to store groundwater.

The geological setting of the study area is generally classified into five classes as (Nn), Quaternary sediments (Q), and quaternary volcanic (Qr, Qd, and Qb) as shown in figure 3.10 below. The major area of the study area was fell under quaternary volcanic (Qd) and (Nn) as was displayed in the figure below.

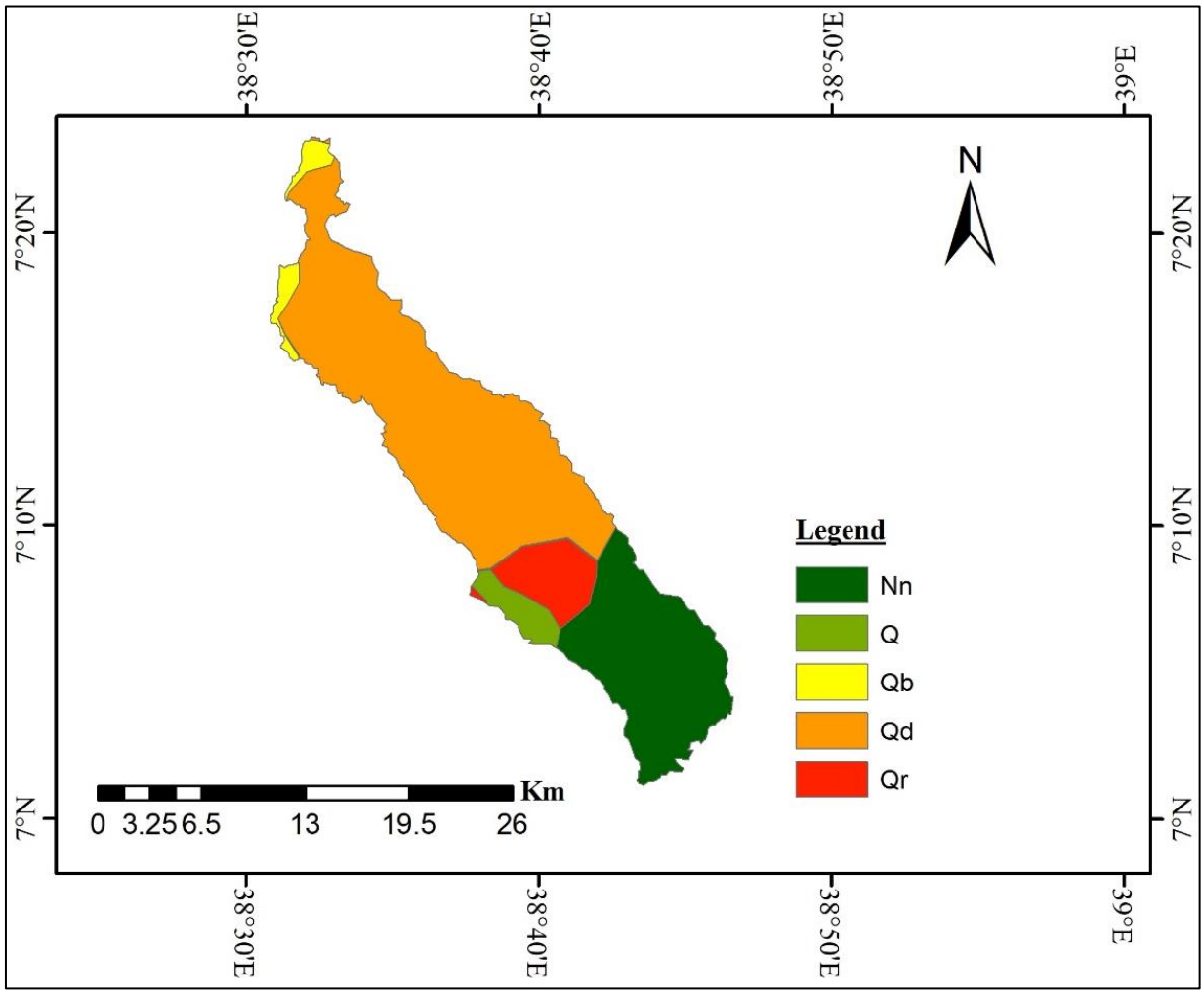

Figure 3. 10: Geological map of the study area

Once the map was prepared in the required manner, a geology thematic layer was developed with classes for appropriate groundwater potential mapping as recommended by (Dainelli et al., 2001; Stefano et al., 2002).

Table 3. 11: Geology classification for groundwater potential zoning

Geology classes	Classes for groundwater potential zoning	remarks
(Nn)	Very high (highly permeable)	5
Quaternary sediment (Q)	High	4
Gademotta Rhyolite Dino formation (Qd)	Moderate	3
Bulbula Lacustrine deposits (Qb)	Low	2
Corbetti pumice flow and fall deposit (Qr)	Very low	1

(Nn): it consists of ignimbrites, unwelded tuffs, ash flows, rhyolites, and trachytes.it is a jointed and faulted rock type and considered a highly permeable formation Quaternary sediment (Q)**:** consists of sandy gravel to mud and it is an aquifer with intergranular permeability. Good permeability at the sand layer and aquiclude at clay. Generally, it is grouped as a well permeable aquifer. Quaternary volcanic) (Qr, Qd and Qb)

(Qd and Qb) Represented by lacustrine, fluvial-deltaic, and colluvial deposits uncomfortably overlying older deposits.

Lacustrine deposits (Qb): consists of a thin alternation of pumices sand, silt, and mud. It is considered as shore sand and reworked pumice. It is grouped in low permeability rocks.

Gademotta Rhyolite Dino formation (Qd): consists of white to blueish gray rhyolite lava flow and tuffs, white pumice, and hard tuffs including obsidian blueish gray rhyolite lava flow. It's an aquifer fractured and grouped as moderately permeable.

Corbetti pumice flow and fall deposit (Qr): consists of a rhyolite lava flow, pumice falls, pumice flow deposit and obsidian lava flow with fracture permeability and it has low permeability.

3.2.1.9 Analytical hierarch process

After all, the thematic layers of each parameter were prepared, the layers would be reclassified to a common scale giving higher values to more Suitable attributes and low value to the less suitable attributes. Reclassifying slope, soil, landuse/land cover, geology/rock type, drainage density, and lineament density, geomorphology and rainfall were analyzed in the ArcGIS environment. The present study analyzes the reclassified layers by giving weight values to each reclassified data sets according to their influence in the suitability model and combines them to delineate the groundwater potential zone of the area. The weight of the parameters can be deriving using weight overlay analysis. By assigning percentage influence (%) of parameters, and comparing the relative importance of criteria. Finally, to arrive at the groundwater potential map and all the thematic layers were overlaid using the weightage overlay module in Arc GIS 10.4. Once the thematic layers were reclassified in the required manner, the Saaty;(2008) approuch was applied to assign weight values for each class for appropriate groundwater potential mapping. To determine the relative importance or weights of each thematic map with another paired comparison matrix was prepared by pair-wise comparison on Satty's importance scale using Microsoft excel 2016. These matrices have the property of consistency known as consistency ratios (CR). Satty indicates that the matrices with CR ratings greater than 0.1 should be re-evaluated. In this case, the consistency value was 0.067 which is accepted. The weights were normalized by multiplying with 100 to avoid complexities of computation.

Table 3. 12: Pair-wised comparison matrix

Criteria	Rainfall	geology	Landforms	slope	Lineament	Drainage	LULC	Soil
Rainfall	1	1	5	2	4	4	3	3
geology	1	1	5	2	3	4	2	2
Landforms	1/5	1/5	1	1/4	1/3	1/3	1/4	1/4
slope	1/2	1/2	4.00	1	5	1/3	1	1
Lineament	1/4	1/3	3	0.2	1	0.33	1	1
Drainage	1/4	1/4	3	3	3	1	0.20	0.20
LULC	1/3	1/2	4	1	1	5	1	1
Soil	1/3	1/2	4	5	1	5	1	1
Sum	3.866667	4.283333	29	14.4803	18.33333	19.99667	9.45	9.45

Table 3. 13: Normalized pair-wised comparison matrix

Criteria	RF	Geo	Geom.	slope	Lin.	Drain.	LULC	Soil	weight	% weight
RF	0.26	0.23	0.17	0.14	0.22	0.20	0.32	0.32	0.23	23.2
Geo.	0.26	0.23	0.17	0.14	0.16	0.20	0.21	0.21	0.20	19.9
Geom.	0.05	0.05	0.03	0.02	0.02	0.02	0.03	0.03	0.03	3.0
Slope	0.13	0.12	0.14	0.07	0.27	0.02	0.11	0.11	0.12	11.9
Lin	0.06	0.08	0.10	0.01	0.05	0.02	0.11	0.11	0.07	6.8
Drain.	0.06	0.06	0.10	0.21	0.16	0.05	0.02	0.02	0.09	8.6
LULC	0.09	0.12	0.14	0.07	0.05	0.25	0.11	0.11	0.12	11.6
Soil	0.09	0.12	0.14	0.35	0.05	0.25	0.11	0.11	0.15	15.0
sum										100.0

Geo = Geology, Slope = Slope, Geom. = Geomorphology/Land form, Soil = Soil, Lin = Lineament density, Drain = Drainage, LULC = Landuse/ Land cover and RF = Rainfall.

4.1.2 Data integration in GIS environment

The present study delineates groundwater potential zones by considering essential parameters and the maps were prepared for each layer. These maps were converted to raster data sets having the same pixels size and different weightage were assigned as per their groundwater potential controlling capacity within the study area and reclassification of each map was done based on the weight values produced and its final ranking and final weighting for each theme are shown in (Table 3.14)

Table 3. 14: Final ranking and final weightage value for each class

Factors	Class	Groundwater prospects	Rank in Number	Influence Weight (%)
Geomorphic units	Plain	very high	5	3
	Valley	high	4	
	Drainage	moderate	3	
	Upper slope	low	2	

	Middle slope ridges	Very low	1	
Geology	Nn	Very high	5	
	Qr	low	1	
	Qd	Moderate	3	
	Qb	Very low	2	
	Q	high	4	19.9
Landuse Land over	Forest Area	Very High	5	
	Agricultural Land	high	4	
	Grassland	moderate	3	
	Bare land	Low	2	11.6
	Built-up Area	Very low	1	
Drainage Density	0-1.87	Very high	1	
	1.87-2.92	High	2	8.6
	2.92-4.68	Moderate	3	
	4.68-5.35	Low	4	
	5.35-6.89	Very low	5	
Lineament Density	0-0.34	Very low	1	
	0.34-0.87	low	2	6.8
	0.87-2.66	Moderate	3	
	2.66-3.55	high	4	
	3.55-4.45	Very high	5	
Slope	0-2.882^{o} Gentle	Very high	5	
	(2.882-5.900 ^{o}) Moderate	High	4	
	(5.900-10.292 ^{o}) High	Moderate	3	11.9
	(10.292-16.19 ^{o}) Steep	low	2	
	(16.19-34.99^{o}) Steep	very low	1	
Soils	Sandy clay loam	moderate	3	
	Clay	low	1	15
	Sandy clay loam	moderate	3	
	Loam	High	4	

	Sandy loam	Very high	5	
Rainfall	1096.85-1214.08mm	Very high	5	23.2
	977.72-1096.85mm	High	4	
	862.38-977.977.72mm	Moderate	3	
	784.86-862.38mm	low	2	
	731.91-784.86mm	Very low	1	

3.2.1.10 Groundwater potential

To determine areas having groundwater resources, a weighted overlap mathematical model was used. After groundwater potential map was developed using weighted index overlay analyses and then the groundwater potential index was calculated using a weighted linear combination method (Malczewski, 1999) Eq.3.5.

$$GPI = G_w G_r + L_{Uw} L_{Ur} + L_{dw} L_{dr} + S_{gw} S_{gr} + D_{dw} D_{dr} + R_w R_r + S_w S_r + G_w G_r \ldots\ldots\ldots\ldots 3.5$$

where, $GPI, G_w G_r, L_{Uw} L_{Ur}, L_{dw} L_{dr}, S_{gw} S_{gr}, D_{dw} D_{dr}, R_w R_r, S_w S_r, G_{mw} G_{mr}$ is groundwater potential index, geology, landuse, lineament density, slope gradient, drainage density, rainfall, soil, and geomorphology, and where the subscripts w and r refer to the weight of a theme and the rate of individual features of a theme, respectively

3.2.2 Groundwater recharge estimation

To achieve this objective, rainfall, temperature, wind speed, soil, slope, groundwater depth, landuse, potential evapotranspiration, and topography data were used to develop grid layers, and for further analyses using the water balance based method the WetSpass model (Esayas and Gebeyehu, 2019: Gebremedhin, 2015).

The WetSpass-m model requires all grid maps should be represented by the same row and column as well as similar cell size. In terms of this, the inputs of satellite data and meteor-hydrological data grid maps have similar cell size, columns, and rows which is 24, 34, and 1200m respectively. All meteorological grid maps were prepared on monthly basis. The rest of the necessary maps were no change and assumed to be constant. Therefore, soil, groundwater depth, slope, topographic elevation, and landuse/land cover maps are the same throughout the year.

The above-listed grid layers were considered in this study as they were widely used in similar studies in various parts of the world (Batelaan and DeSmedt 2001:Batelaan and DeSmedt, 2007). The following sub-sections are provided as to how these grid layers were generated and how the WetSpass model was applied to estimate groundwater recharge for the study area.

3.2.2.1. Rainfall

As explained in section 3.2.1.1 above, the source, method of data analysis was the same but the only difference was for groundwater potential mapping the mean annual rainfall is used but for this specific objective long-term average monthly rainfall was used (Appendix 7.4). The other difference was that the format of map preparation and was prepared in grid map by the IDW with batch processing interpolation method in ArcGIS environment and taken as grid map (ASCII file format) for later model input. The long-term average monthly rainfall distribution in and around the watershed is shown in Figure 3.11.

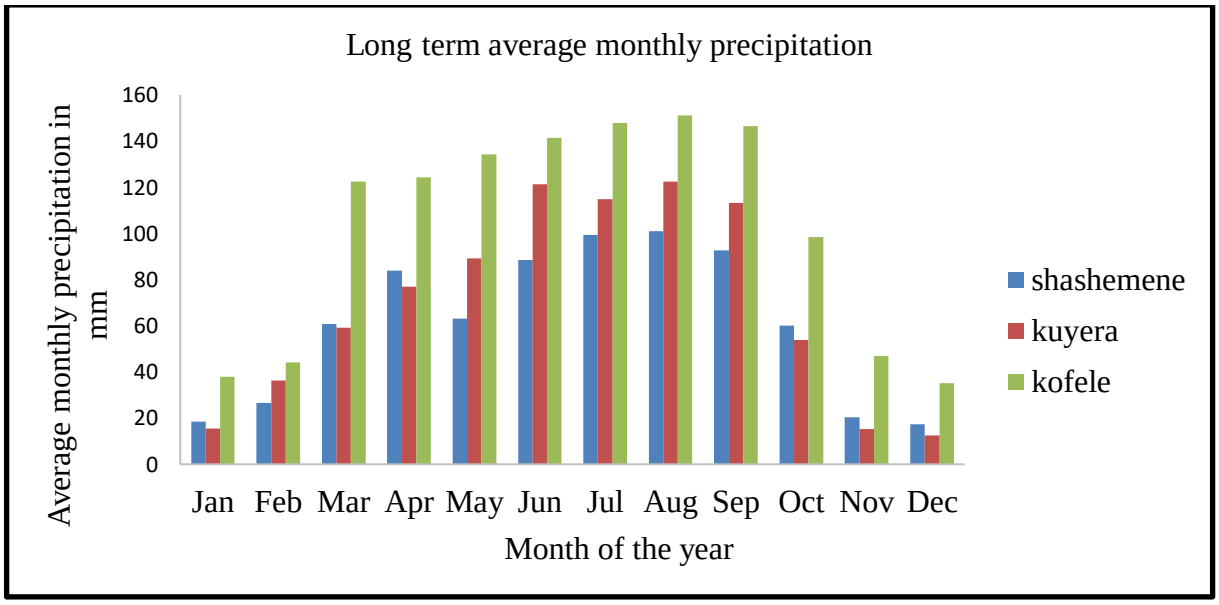

Figure 3. 11: Monthly rainfall for stations in and around the study area

Using the IDW interpolation with batch processing the rainfall of the study area is presented as follows and it was converted to ASCII file format to make the map have the same column and row.

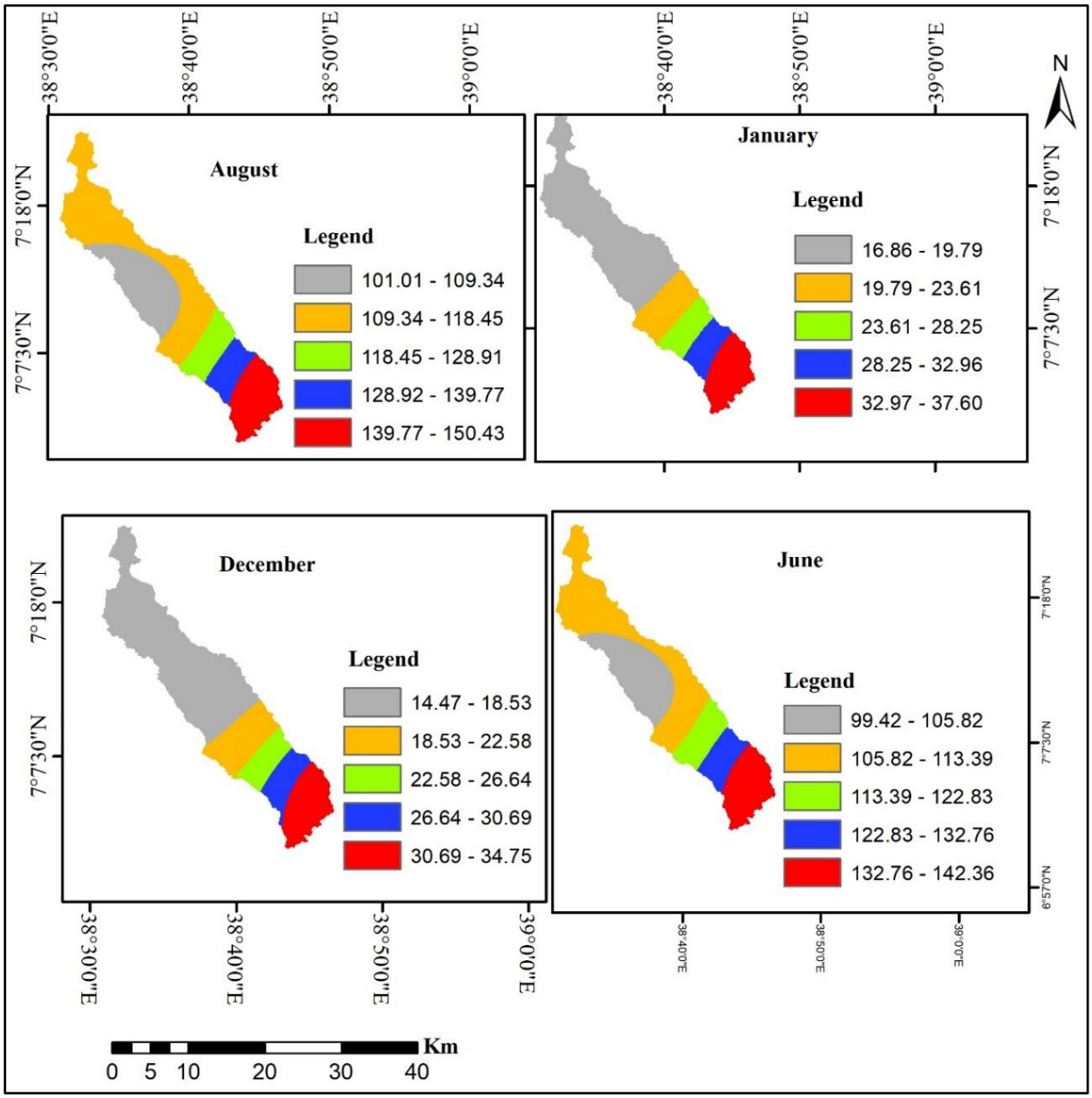

Figure 3. 12: Long term average monthly rainfall Melkaoda watershed sample months

3.2.2.2 Temperature

Temperature data of three meteorological stations, which are found in and around the study area were collected from the Ethiopia National Meteorology Agency and the data are presented in Appendix 7.4. The grid map was prepared using ArcGIS then IDW with batch processing interpolation method and then the map has taken as a grid map (ASCII file format) for later model input. Its long-term average monthly temperature in and around the study area is shown in Figure 3.13 below.

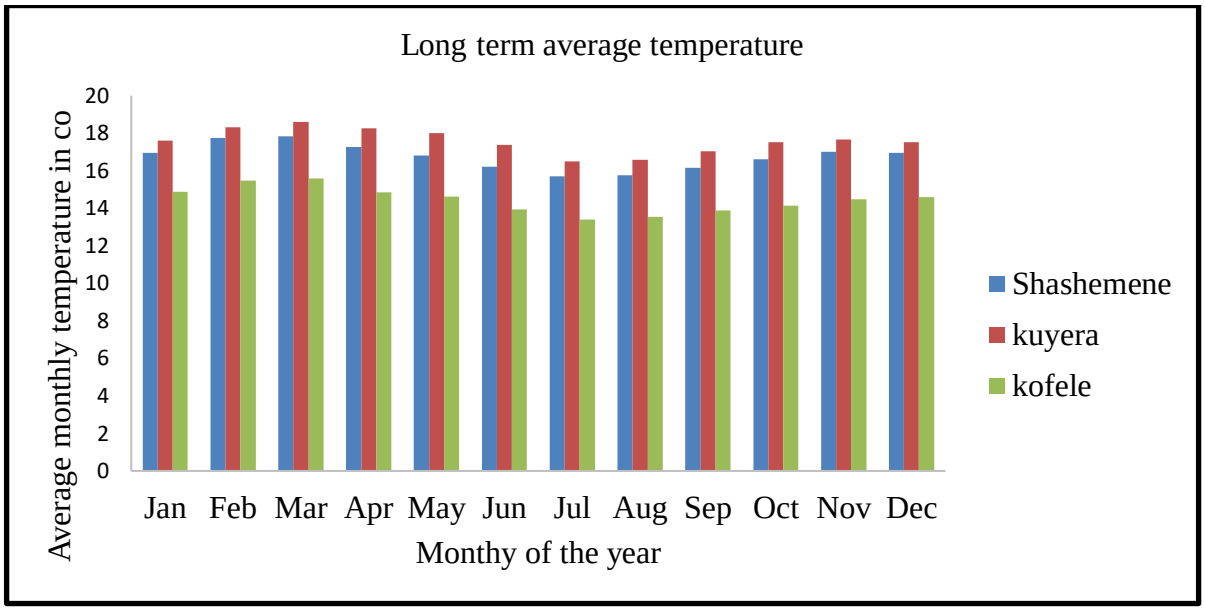

Figure 3. 13: Monthly average temperature value of surrounding stations

Using IDW interpolation with batch processing temperature map is also prepared and then it was converted to ASCII file format. The long-term average monthly temperature value ranges between 14.49c^{o} and 17.256c^{o} throughout the year with a mean of 15.997c^{o}.

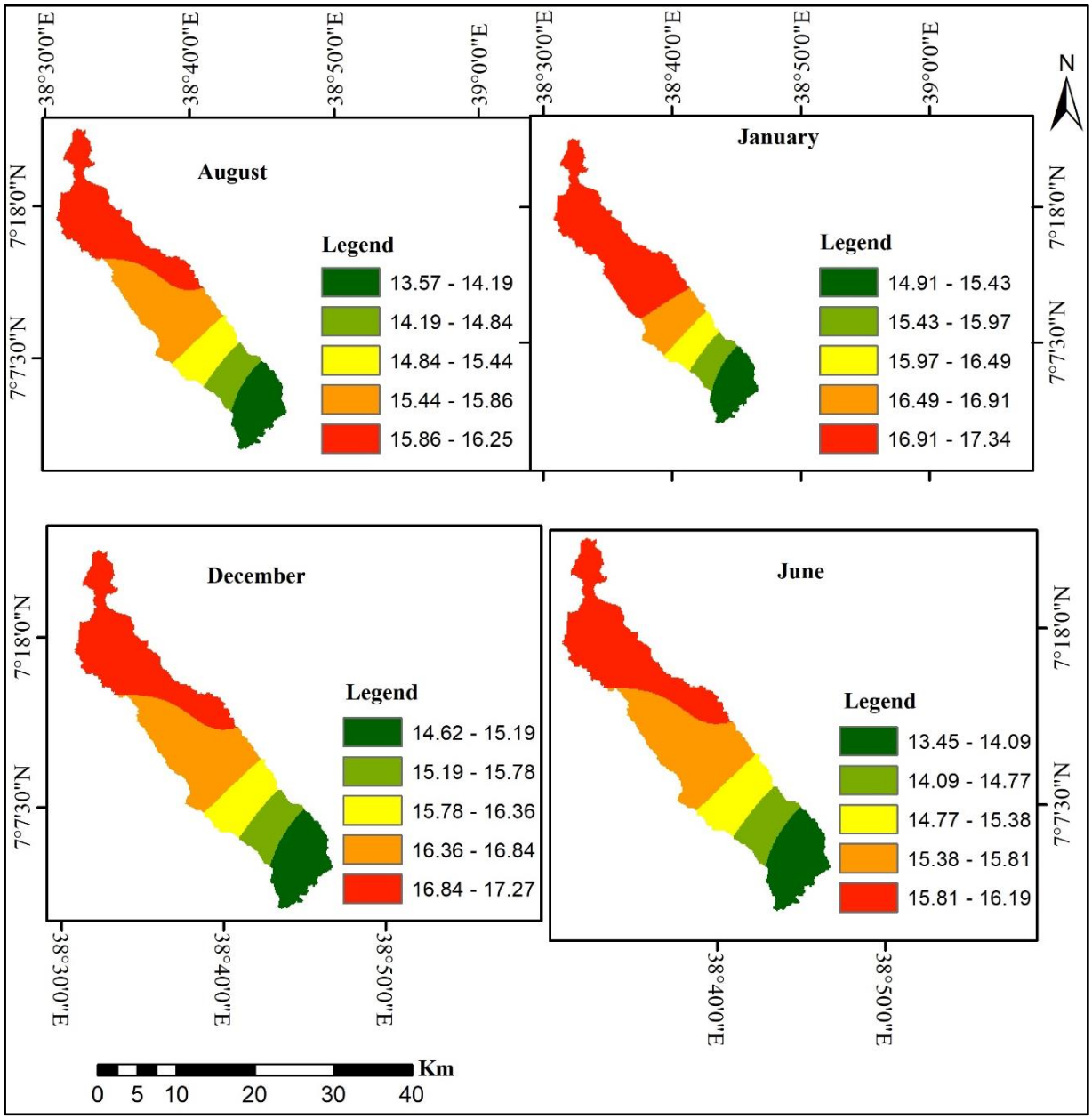

Figure 3. 14: Long term average monthly temperature Melkaoda watershed

3.2.2.3 Potential evapotranspiration

To develop a potential evapotranspiration map of the study area, the three meteorological (wind speed, solar radiation, and maximum and minimum) data for this task were collected from the Ethiopia National Meteorology Agency and calculated using the Penman-Monteith method then the obtained result was prepared in a required manner and then its map was prepared in grid file

by IDW with batch processing interpolation method in ArcGIS environment and taken as grid map (ASCII file format) for model input.

The monthly PET of the Melkaoda watershed is calculated using the Penman formula. The monthly results were changed into average monthly potential evapotranspiration. Finally, the calculated average monthly PET values of each month were converted to spatially distributed grid maps using IDW interpolation techniques with batch processing. The grid maps of PET for monthly bases were used with other input parameters in the WetSpass-m model. The obtained result for sample months is shown below in figure 3.15. The long-term monthly average PET ranges between 238.466 mm to 273.82 mm with a mean value of 256.99mm then converted to ASCII file format for the simulation of the model.

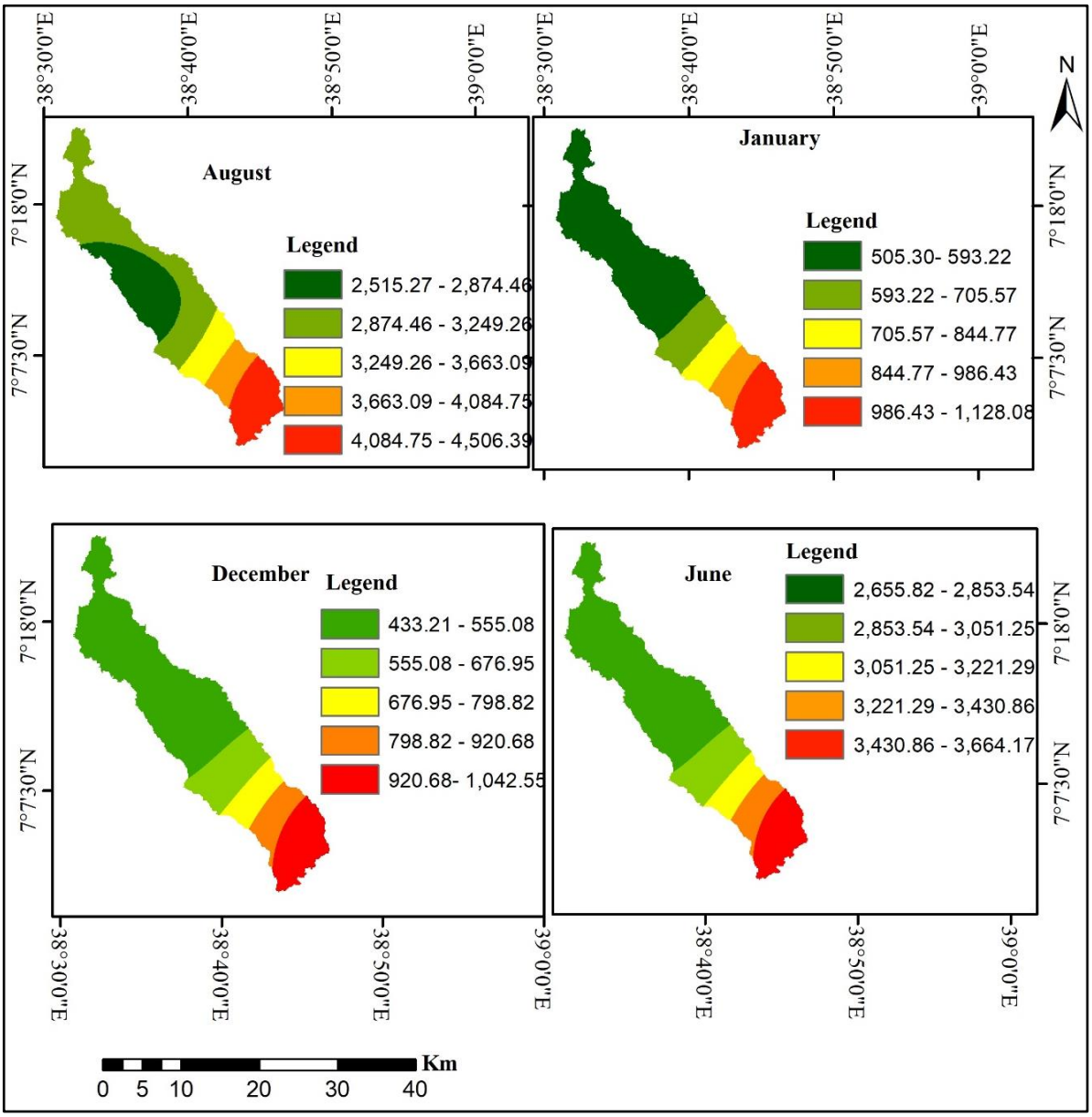

Figure 3. 15: Long term average monthly PET Melkaoda watershed sample months

3.2.2.3 Wind speed

To develop a grid map of wind speed, wind speed data of three meteorological stations found in and around the study area were collected from the Ethiopia National Meteorology Agency and the data are presented in Appendix 7.1. The grid map was prepared using ArcGIS then IDW with batch processing interpolation method was applied and then the map has taken as grid map (ASCII file format) for later model input. Its long-term average monthly temperature in and around the study area is shown in Figure 3.16 below.

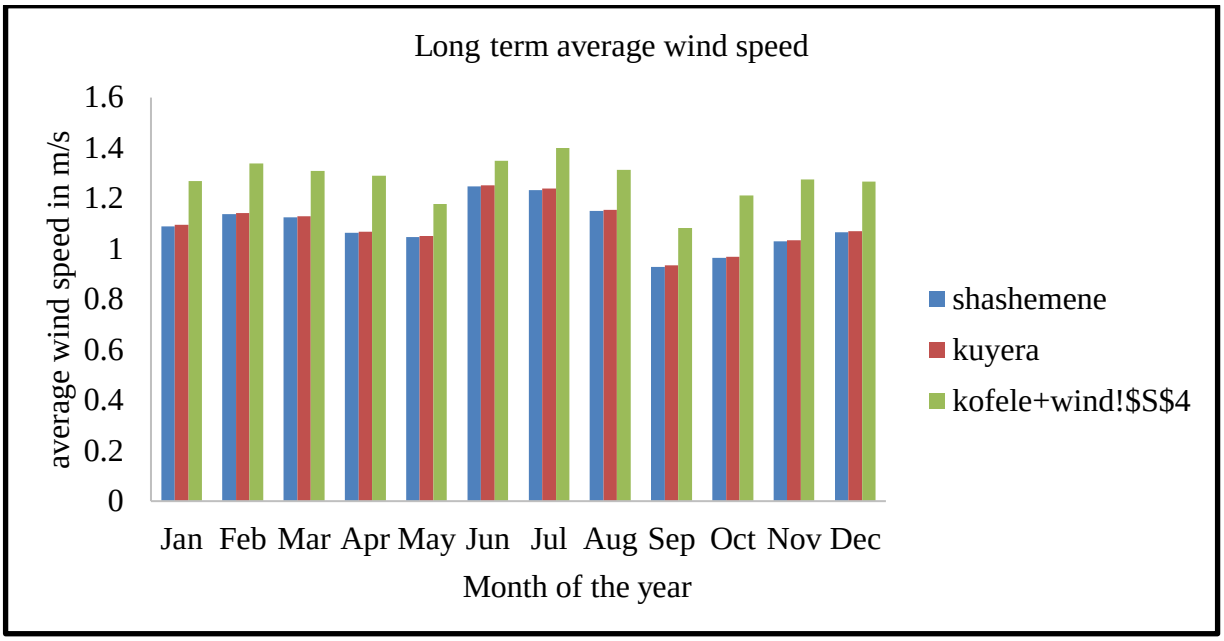

Figure 3. 16: Monthly average wind speed value in and around Melkaoda Watershed

After a long term, the monthly average value of wind speed was calculated from daily obtained data from the meteorological agency of Ethiopia and the values of each station were interpolated and converted to a grid map using the IDW interpolation method. This grid map of wind speed for average monthly was converted to ASCII file format and used as input parameters in the WetSpass-m model.

The long-term monthly average wind speed ranges between 1. 09 m/s and 1.27m/s with the mean of 1.17 m/s as interpolation result shows in Figure 3.17 for sample months.

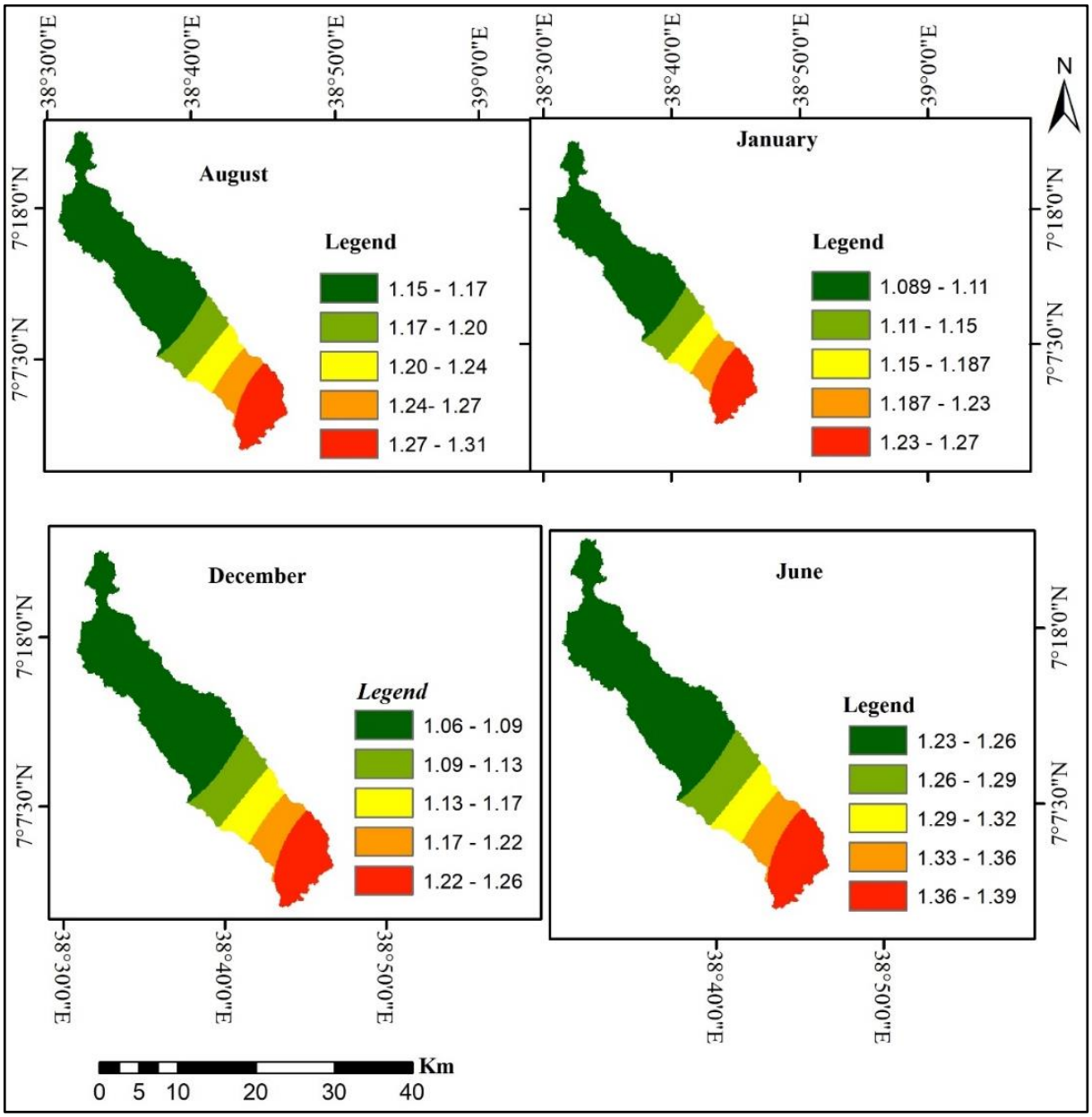

Figure 3. 17: Long term average monthly wind speed Melkaoda watershed sample months

3.2.2.4 Groundwater depth

To develop a grid map of groundwater depth, groundwater depth data of six boreholes found in the study area were collected from the West Arsi Zone water mineral and energy office and depth was calculated by subtracting static water level (SWL) from the ground surface level (Appendix 7.7.2). After driving the groundwater depth of the study area, the map was prepared in grid file format by using the IDW interpolation technique in the ArcGIS 10.4 environment.

The groundwater depth has been calculated by deducting static water level from ground surface level and its map was produced. These data were interpolated using ArcGIS IDW spatial analyst tool to represent the total area of the watershed and then the grid map is converted to ASCII file format for model simulation.

3.2.2.5 Landuse/land cover

As explained in section 3.2.1.2 above, the source, method, and data analysis were the same but the only difference was for groundwater potential mapping the grid map format is used but for this specific objective grid map in ASCII file format is used.

3.2.2.6 Topography

The topography (elevation) map of the watershed was obtained from DEM which is downloaded from the Shuttle Radar Topography Mission (SRTM) dataset of the United States of Geological Survey (USGS) and processed in ArcGIS environment finally the map format was changed to ASCII file format for a further model effective run.

3.2.2.7 Slope

Everything was the same with section 3.2.1.2 above, the source, method of data collection, and data analysis are the same except the map format. For potential mapping, the grid map format is used but for this specific objective grid map in ASCII file format is used.

3.2.2.8 Soil

The source, method of data collection, and analysis were the same with the groundwater potential zone mapping but the file format is the only difference. Its detail is discussed in section 3.2.1.2 above.

3.2.2.9 Parameter tables

Four types of parameter tables are needed to run the model. Those types of parameter tables were prepared in an appropriate format (TBL) for the effective model running process. Landuse parameter table (Appendix 7.5), soil parameters table (Appendix 7.6), and Number of rainy day parameter table (Appendix 7.7) were prepared as attribute lookup tables as an input of the model. These different biophysical data lookup tables are obtained by own processing depending on user guidelines and reviewed from scholarly published pieces of literature. The developed grid

maps and the parameter data together make the required interaction with each other to produce appropriate average values during the simulation processes.

3.2.2.10 Application of WeSpass-m model

Surface runoff

WetSpass-M model calculates the monthly surface runoff SRm in (mm/month) using a rational method applied on a monthly time step using two coefficients:

$$SR_m = C_{sr} C_h (-) \qquad eq.3.6$$

Where C_{sr} an actual runoff coefficient (–) and C_h is a coefficient (–) representing soil moisture conditions (Bahremand et al., 2007):

$$C_h = (\frac{N_s}{N_{sat}})^b \qquad eq.3.7$$

Where N_s is the cell soil moisture content (m3/m3), N_{sat} is the soil porosity (m3/m3) and b is an exponent (–) representing the effect of rainfall intensity. For b = 1, a linear relation between C_h and soil moisture is assumed. (Bahremand et al. 2007) obtained an optimal value for b through calibration using discharge time series. For semiarid regions, where soil moisture is generally low and (potential) evapotranspiration is high, Ch is included in Eq. 3.7 to avoid overestimation of surface runoff. As soil moisture data at the monthly time step is scarce, Ch (between 0 and 1) can be approximated by integrating the evaporative efficiency ratio (Abdollahi et al..,2017) and (Pistocchi et al..,2008).

$$C_h = \frac{P_m}{L_P({P^a}_m + {ET_m}^a)^{\frac{1}{a}}} \qquad if\ ET_m > P_m \qquad eq.3.8$$

$$C_h = 1, ET_m\ if < P_m$$

Where ETm is the potential evapotranspiration (mm/month), LP is a calibration parameter (–) which reduces the potential evapotranspiration depending on the soil moisture (default is 0.65). (Pistocchi et al..,2008) Suggested a value of 1.5 for the exponent as an average value on the monthly scale. The runoff coefficient integrates many factors such as surface roughness, infiltration, and depression storage. Therefore, it is a critical input parameter in water balance modeling. To improve the estimation of the potential runoff coefficient per grid cell, it is calculated from the runoff coefficient for permeable areas (Cper) and the runoff coefficient for

the impervious part (CImp) according to their area. Cper is obtained from a weighted sum of landuse/land cover, soil, and slope factors, respectively

Evapotranspiration

WetSpass computes evapotranspiration per grid cell by summing up actual evapotranspiration from the vegetated (ETV, open water (ETO), bare soil (ETs), and impervious surface (ETi) area fractions. In a similar approach, WetSpass-M uses potential evaporation at a monthly timescale and vegetation coefficients for estimation of actual evapotranspiration. For calculation of the reference transpiration from the potential evapotranspiration (ETP), a vegetation coefficient is required which is estimated as:

$$C = \frac{1 + \frac{\gamma}{\Delta}}{1 + \frac{\gamma}{\Delta}(1 + \frac{r_c}{r_a})} \qquad Eq.3.9$$

Where C is the psychrometric constant (kPa/C^o), which is the gradient of the first derivative of saturated vapor pressure curve (slope of saturation vapor pressure at the temperature of the atmosphere), rc (bulk) surface resistance (s m^{-1}), and ra aerodynamic resistance (s m^{-1})

$$r_a = \frac{1}{k^2 u_a}\left(\ln\left(\frac{Z_a - d}{Z_0}\right)\right)^2 \qquad \text{Eq.3.10}$$

Where K is the von Karman constant (0.41), ua (m/s) is the wind speed at elevation Za (m), Zd is zero displacement elevation (m) and Zo is the aerodynamic roughness height of surface (m). For vegetated groundwater discharge areas, the vegetation coefficient is equal to 1. Therefore, the reference transpiration (Trv) is given by:

$$T_{rv} = cETP \qquad eq.3.11$$

The total actual monthly evapotranspiration per grid cell [ETm (mm/month)] now becomes:

$$ET_m = avET_V + asET_s + aoET_o + aiET_I \qquad eq.3.12$$

Where $_{av}ET_v$, area fraction and evapotranspiration for the vegetated area, $_{as}ET_s$, bare soil $_{ao}ET_o$ open water and $_{ai}ET_i$ is the impervious surface (Batelaan & DeSmedt, 2001) and (Batelaan and De Semdt, 2007).

Recharge

Computation of long-term average spatial patterns of recharge was the main objective for the development of the WetSpass methodology (Batelaan, O., & DeSmedt, F, 2001). In WetSpass-M, monthly recharge [Rm (mm/month)] is calculated as the residual term of the water balance:

$$R_m = P_m - SR_m - ET_m \qquad eq.3.13$$

As recharge is a rather slow process, monthly base-flow for each cell is calculated based on the storage of the previous month and the recharge in the considered month:

$$Q_{b(t)} = BQ_{b(t-1)} + 0.001Nm(1-B)\emptyset Rm \qquad eq.3.14$$

Where B is a storage parameter (–) (between 0 and 1), $BQ_{b(t-1)} - 1$) is the base-flow from the previous month (m^3/month), Nm is the number of rainy days per month, and $\emptyset$ (m^2/day) is the recharge contribution parameter to current base-flow. For grid cell area A (m^2) with recession index k (day).

$$\emptyset = \frac{1.15A}{K} \qquad eq.3.15$$

The groundwater recharge is calculated from the following equation as the residual of the water balance and precipitation, (Aish, 2009).

$$P = I + S_v + ET_v + R_v \qquad Eq.3.16$$

Where P is the average seasonal precipitation [LT-1], I is the interception by vegetation [LT-1], Sv is runoff overland surface beneath vegetation [LT-1], ETv is the actual transpiration [LT-1] and Rv is groundwater recharge [LT-1]. The final duty for the WetSpass model is estimating the spatially distributed groundwater recharge, which can be calculated from the water balance:

$$R_v = P - S_v - ETv - I \qquad Eq.3.17$$

Where p is precipitation, S_v runoff overland surface beneath vegetation is interception by vegetation, and ET_v is the actual evapotranspiration [LT^{-1}] calculated as the sum of transpiration T_v and E_s (the evaporation from bare soil found in between the vegetation).

The spatially distributed recharge is therefore estimated from the vegetation type, soil type, slope, groundwater depth, and climatic variables of precipitation, potential evapotranspiration, temperature, and wind speed.

Water balance per raster cell

The water balance components of the vegetated area, bare-soil, open-water bodies, and impervious land surfaces are used to compute the total water balance of a raster cell for a given

watershed. The total evapotranspiration, surface runoff, and groundwater recharge of a raster cell have been computed using the equations (Eq 3.18, 3.19, 3.20) which had described by (Batelaan, O., & DeSmedt, F, 2001).

$$ET_c = a_v ET_v + a_s E_s + a_o E_o + a_i E_i \qquad Eq.3.18$$

$$S_c = a_v S_v + a_s S_s + a_o S_o + a_i S_i \qquad Eq.3.19$$

$$R_c = a_v R_v + a_s R_s + a_i R_i \qquad Eq.3.20$$

where ET raster, S raster, and R raster are the total evapotranspiration, surface run-off, and groundwater recharge of a raster cell, respectively, each having a vegetated, bare-soil, open-water, and impervious area component denoted by a_v, a_s, a_o, and a_i, respectively. The indices v, s, o and i stand for the vegetation area, bare area, open water area, and impervious surfaces, respectively. S_v, S_s, S_o, and S_i are the surface run-offs in vegetation area, bare area, open water area, and impervious surface, respectively. E_v, E_s, E_o, and E_i are the evaporations in vegetation area, bare area, open water area, and impervious surface consequently. R_v, R_s, R_o, and R_i are the groundwater recharges in vegetation area, bare area, open water area, and impervious surface, respectively.

3.2.2.11 Model calibration

The total flow in a stream or river from a watershed is a function of Qbase flow and Qsurface runoff which is equivalent to the long-term monthly average river discharge from the watershed (Abdollahi et al., 2017).

Model Calibration result was performed based on manually adjusting different parameters placed on the model with range values. The parameters are namely: alfa coefficient, “a” interception, Lp coefficient, and runoff delay factor “x”. The parameters were kept optimizing up to reaching the goodness of fit between the simulated and observed stream discharge recorded at Melkaoda river gauge station.

Water resource studies highly depend on streamflow data. Daily streamflow data for Melkaoda River from 2004 to 2018 GC is collected from the Ministry of Water, Irrigation, and Electricity of Ethiopia, and this data was used for calibration purposes to analyze the estimation of groundwater recharge.

The total flow in a stream is a function of Qbase flow and Qsurface runoff.

$$Q_{total} = Q_s + Q_b \qquad Eq.3.21$$

Where, Q_{total}(m^3/month), Q_s (m^3/month), Q_b (m^3/month) total streamflow in the river, simulated surface runoff, and simulated base flow respectively.

Model performance evaluation

To evaluate the model simulation outputs relative to the observed data, model performance evaluation is necessary. There is a various method to evaluate the model performance during calibration and validation periods. For this study coefficient of determination (R^2), Nash and Sutcliff simulation efficiency (NSE), and PBIAS were used.

The determination Coefficient describes the linear relationship between simulated and observed data. Its value ranges from zero to one. A higher value close to 1 indicates good co-relation and typically values greater than 0.6 are considered acceptable (Santhi et al.., 2001).

$$R2 = \frac{[\sum(Qo - mean.Qo)(Qs - mean.Qs)]2}{\sum(Qo - mean.Qo)2 \ \sum(Qs - mean.Qs)2} \quad \text{(3.22)}$$

The Nash and Sutcliffe simulation efficiency indicates how well the plots of observed versus simulated data fit the 1:1 line. The value ranges from negative infinity to one. Values greater than 0.5, indicate the simulated value predicted better. A value greater than 0.5 is acceptable performance (Santhi et al., 2001).

$$NSE = 1 - [\frac{\sum(Qo - Qs)2}{\sum(Qo - Mean.Qo)2}] \quad \text{(3.23)}$$

The proportion of PBIAS describes the tendency of the simulated data to be greater or smaller than the observed data, expressed as a percentage. The optimum PBIAS value is zero and low indicates that the model simulation is satisfactory. Positive values indicate a tendency of the model to underestimate while negative values indicate overestimation (Moriasi, 2007).

$$PBIAS = [\frac{\sum(Qo - Qs)}{\sum Qo}] \quad \text{3.24}$$

3.2.3 Impacts of landuse/land cover on groundwater recharge

To achieve this objective, all methods and data used in this section were the same as the methods, data stated, and used in section 3.2.2 of the above. In this case, all variables were assumed to be constant except landuse/land cover of the year1989.

3.2.3.1 Landuse/land cover of 1989

To develop the landuse/land cover map of the study area, a satellite image of the study area for the year 1989 from Landsat-5 Enhanced thematic mapper (ETM^+) was downloaded from the

USGS website. The downloaded satellite image was processed using ERDAS imagine by carrying out the process like layer stacking, sub-setting the study area from a stacked image, and then it was classified using the supervised classification technique. After preprocessing finished, image classification was done then accuracy assessment of classified images was done for verification and validation of the results as described in section 3.2.2.2 above for the year 2018. Finally, landuse/land cover classified into five classes as the same as it has done for the year 2018 with the overall accuracy assessment of 89% that has a strong agreement with (Anderson, 1997) and kappa hat coefficient of 0.839 that has a strong agreement with (Foody, 2002).

LULCC detection

The process of identifying differences in the LULC of the Melkaoda catchment was done by observing the classified images at different times (1989 and 2018). Therefore, comparisons based on two satellite images of 1989 and 2018 were made. To achieve this, the first task was developing a table showing the area, percent, and changes between the periods of 1989 and 2018 measured for each LULC. Temporal change and rate of change were also computed to demonstrate the magnitude of the changes experienced.

$$Temporal\ LULCC(\%) = \frac{Area\ at\ final\ Yr. - Area\ at\ initial\ Yr.}{Area\ at\ initial\ Yr.} * 100 \quad \text{..... (3.25)}$$

$$Rate\ of\ change\ = \left(\frac{Final\ Area\ at\ Final\ yr. - Area\ at\ Initial\ Yr.}{Area\ at\ initial\ Yr.} * 100\right) * 1/T \quad \text{..... (3.26)}$$

where T is the difference in time between two periods.

To evaluate the variability of groundwater recharge due to LULCC, the two LULC (1989 and 2018) maps were used independently in the two simulations while keeping other variables constant. The study then discovered the annual variation of groundwater recharge due to the LULC map of 1989 and 2018. The detailed procedures to estimate recharge for the two periods (1989 and 2018) were explained in the same for the two years as discussed in section 3.2.2 in this chapter.

To quantify the impacts of landuse change on groundwater recharge in the Melkaoda watershed, the WetSpass-m model used to estimate the quantity of recharge, runoff, and evapotranspiration under different landuse areas in two scenarios as is shown in figure 3.18 below.

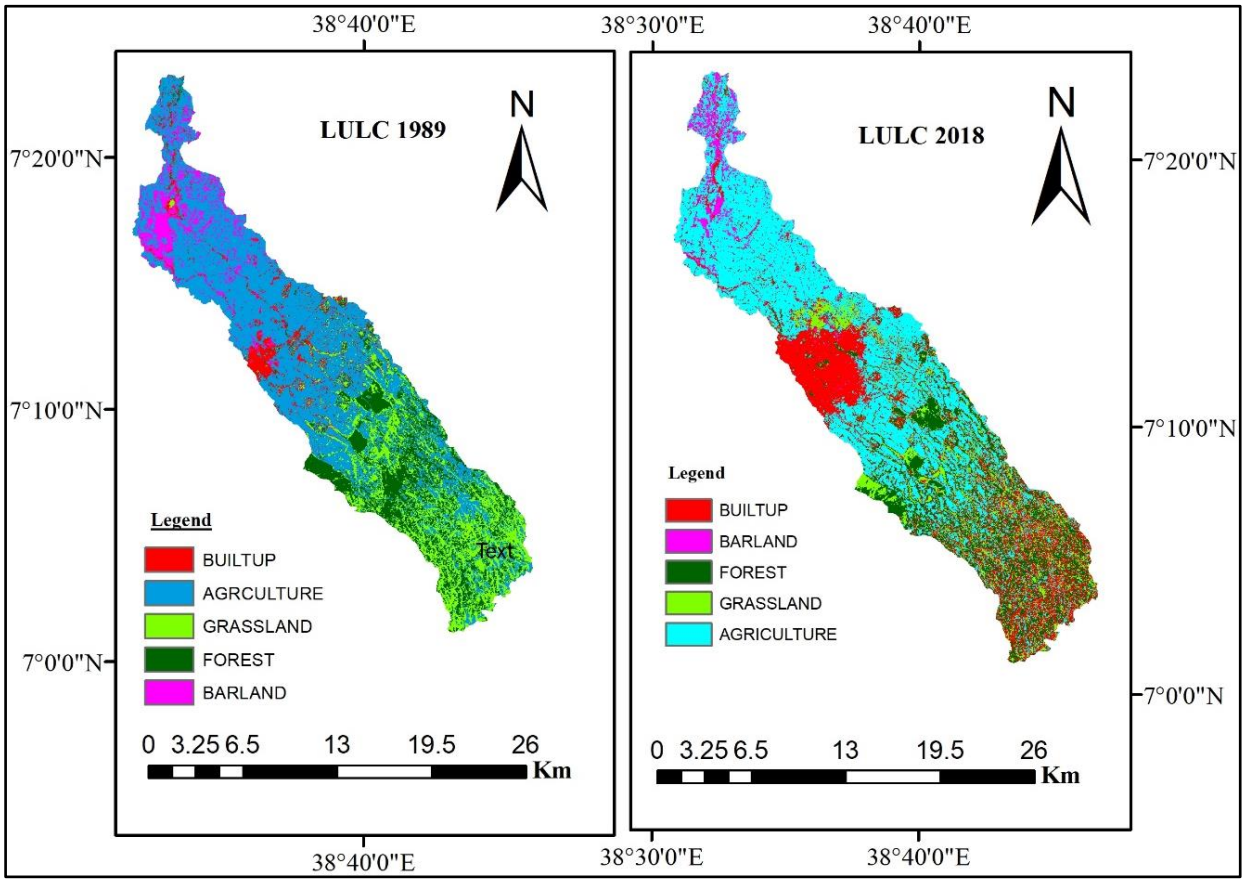

Figure 3. 18: Maps of land cover changes in Melkaoda watershed in 1989 and 2018

The LULC analyses showed that the occurrence of LULCC in the Melkaoda watershed. The result was shown in the percent of temporal change and rate of change in table 4.5.

Table 3. 15: Area of LULCC, temporal changes, and rate of change

LULC classes		AGRL	BRL	FRST	GRL	BTUA	sum
Area in Km2	1989	159.00	25.03	56.13	58.27	16.57	315
	2018	161.18	11.00	46.02	27.21	69.60	315.
Area in percent	1989	53.65	6.36	17.18	17.86	4.94	100
	2018	47.99	3.49	14.61	8.64	25.27	100
Temporal change (%)	1989-2018	1.37	-56	-18.06	-53.3	76.65	
Rate of Change (% /yr	1989-2018	0.046	-1.87	-0.602	-1.78	2.56	

The major LULCC trend observed includes a decline in bare land, forest, and grassland, and expansion of agricultural land and built-up areas. Agricultural land which has always comprised the largest portion of the watershed area increased slightly between 1989 and 2018. During this

period the built-up area has increased considerably by 76.65 percent. Note: Built-up includes urban areas and rural settlements in the landuse classification stated above

According to (Gurnell et al.., 2016), the presence of vegetation increases the infiltration of water (via roots) and decreases soil evaporation, which coincides with the research of (Jinno et al.., 2009), because as the urbanization stretches over increasingly larger areas, the ecological environment cannot be guaranteed.

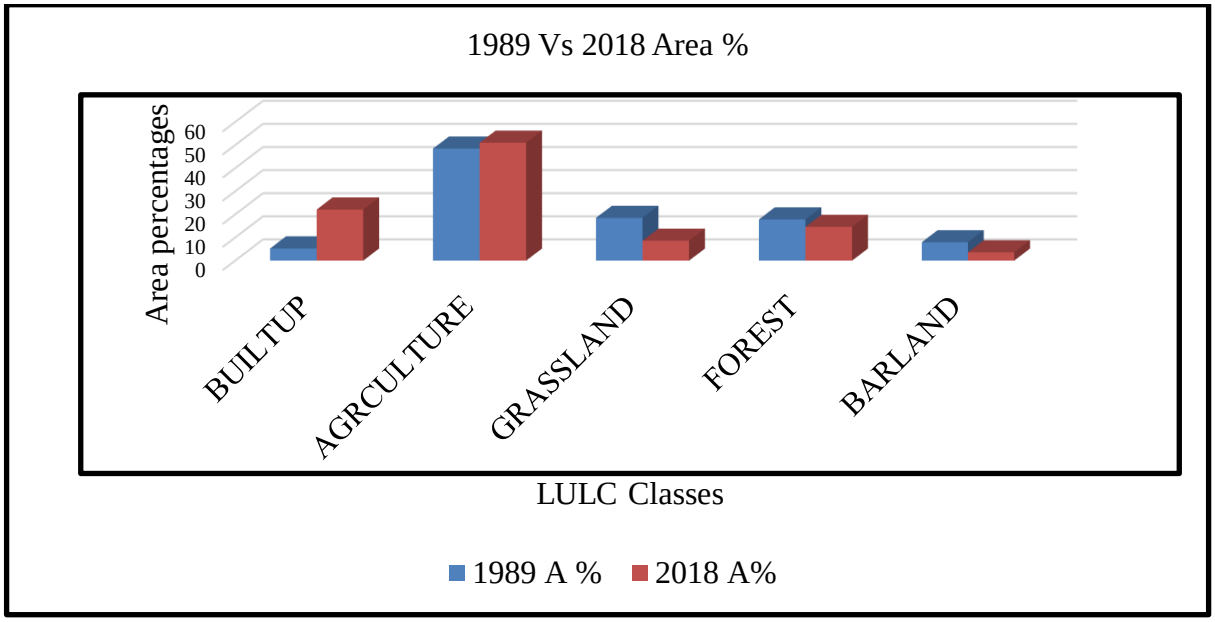

Figure 3. 19: Area percentage of different landuse types in 1989 and 2018

3.3 General framework of the study

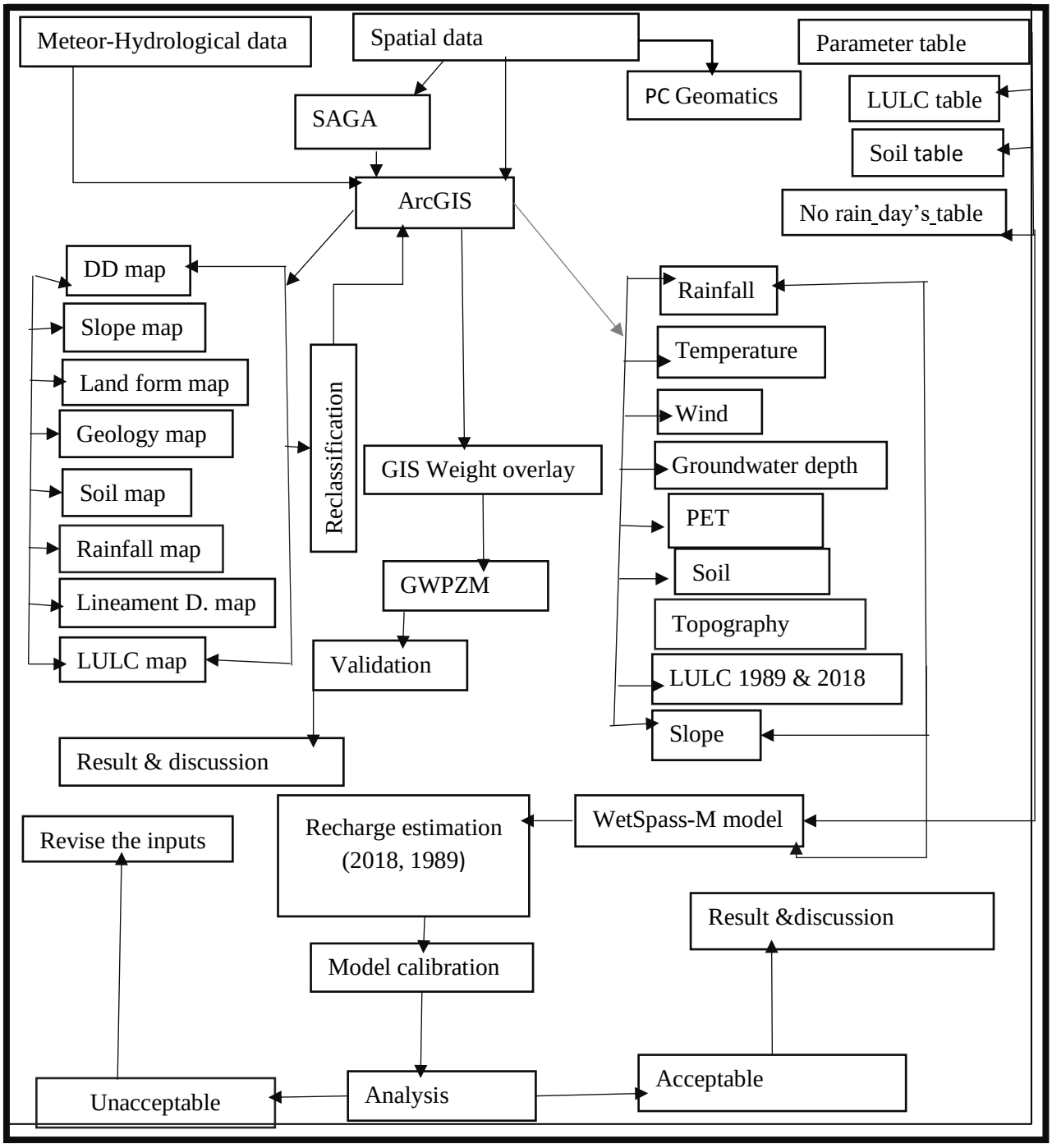

Figure 3. 20: Flow chart depicting general work of this research

4. RESULTS AND DISCUSSION

4.1 Groundwater potential mapping

4.1.1 Groundwater potential zone

The identification of groundwater potential zones for the study area was made by grouping the interpreted layers through Weighted Overlay Analysis and finally assigned different potential zones. Depending upon the groundwater potentiality, each class of the main eight thematic layers (geomorphology, slope, geology, drainage density, lineament density, soil, landuse/land cover, and rainfall) were placed into one of the following groups viz., 1.very high, 2. High, 3. Low, 4. Very Low.

A final groundwater potential map is prepared with the application of the above technique. Most of the regions in the study area concern a good level of groundwater potential zone.

From the composite layer, the delineation of groundwater prospect zones was made by grouping the polygons into different prospect zones: Very high, High, low, and very low. The prospect map describing the groundwater potential zone in the study area was identified and presented in (Figure 4.1). From this study, Groundwater potential zones were categorized into four types as very low (0.069 %), Low (28.790%), High (52.764%), and Very High (18.377%). In the study generally, the reason for very high groundwater potential was the area that has low drainage density, low slope, and very high rainfall, and (Nn) geological formation. The reason for Low groundwater potential zone is an area that has high drainage density, high slope, and low lineament density, high ridges geomorphological units, urban area.

The study suggested that the GWPZM generated was served as useful guidelines for planners, engineers, and decision-makers providing quick decision-making in the management of groundwater resources, site selection for GW exploration and exploitation.

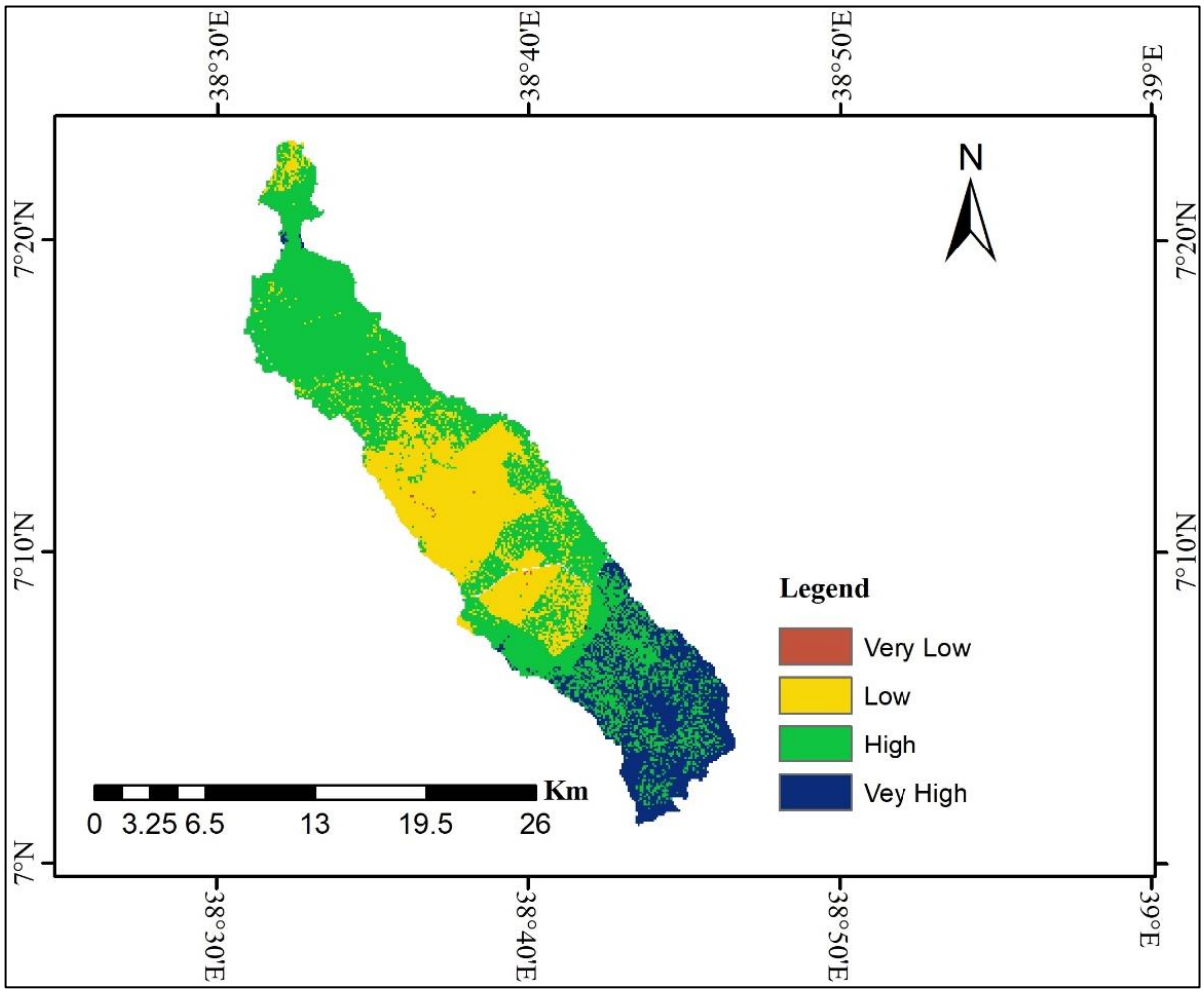

Figure 4. 1: Groundwater potential zones map

Table 4. 1: Groundwater potential zones map

Sr. No	Groundwater Potential zones	Area in (Km^2)	Area in (%)
1	Very Low	0.216	0.069
2	Low	90.688	28.790
3	High	166.2048	52.764
4	Very High	57.8872	18.377
Total		315	100

4.1.2 Result validation

There is the comparison of the study between the water level depth data and the groundwater potential zones map was done by (Kavitha et al., 2011). It was found that the delineation of groundwater potential zone by integrated GIS and remote sensing techniques was in close

agreement with the available point source inventory data shown in (Appendix 7.9). Borehole data like groundwater depth, borehole wells points, and borehole discharged/yields (m3/h) was obtained from Shashemene town water supply bureaus and is used for model validation purpose Classification of each potential zone is based on JMG generalized groundwater potential classes, i.e., very low, low, high, and very high (JMG., 2007). Map overlay between predicted groundwater potential map and Groundwater storing controlling parameters found that the area having high and very high groundwater potential included the flat area of the slope, low drainage density, high lineament density, and high rainfall, and geological area of high permeability.

Flat areas of slope and low drainage density are favorable to groundwater potential due to the high infiltration rate. (Musa, 2000) only found two factors related to the high potential of groundwater which is low drainage density and high lineament density. Lastly, low groundwater potential zones include geomorphology types of high ridges, high drainage density, steep slope degree, low annual rainfall intensity, soil type of clay, and landuse type of clear land and urban areas.

The accuracy of the GIS model of the predicted groundwater potential map was determined with the existing groundwater borehole wells compiled by the JMG (Table 4.2).

The borehole wells data used to validate the predicted groundwater potential with the existing groundwater potential is collected from the Shashemene town water supply office. From the data presented for groundwater borehole wells, there are 6 borehole wells with the yield ranging from 6.67-18m^3/h. The minimum deep of borehole wells is 159m and the maximum is 311m. The average deep of borehole wells is 209.975m. The mean yield of borehole wells in the study area is 13.038m^3/h. It falls under the JMG groundwater potential classification as “high potential yield” (19 m3/h).

Model validation of predicted groundwater potential zones with the groundwater borehole wells data shows 100% of accuracy that all six wells correctly agreed with predicted groundwater potential zones. It means that generated groundwater potential map has a good agreement with the groundwater borehole wells. The details are shown in (Table 4.2) and Figure 4.2 below.

Table 4. 2: Model validation using groundwater borehole wells

Well no.	T/source	Depth	Discharge(L/s)	Yield(m3/h)	JMG Classification	Predicted GWPZ	Validation
1	DW	180	2.86	10.3	High(10-19m3/h)	High	correct
2	DW	159	1.86	6.67	High(5-9m3/h)	Low	correct
3	DW	311	2.95	10.62	High(10-19m3/h)	High	correct
4	DW	277	5	18	High(10-19m3/h)	High	correct
5	DW	168.6	4.26	15.34	High(10-19m3/h)	High	correct
6	DW	164.25	4.8	17.3	High(10-19m3/h)	High	correct

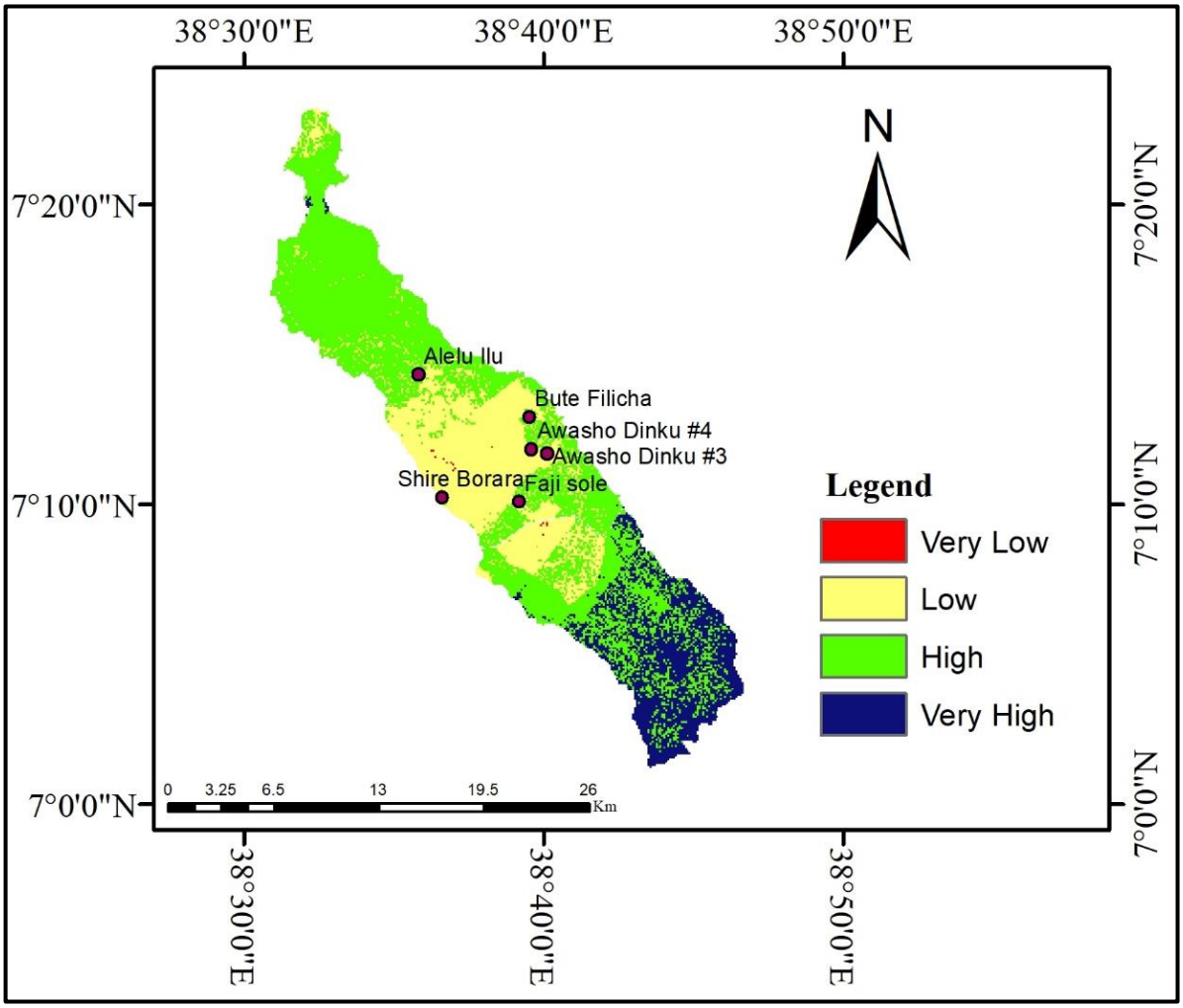

Figure 4. 2: Predicted groundwater potential zones map overlapped with borehole

4.2 Recharge estimation

4.2.2 Model calibration

The summation of baseflow and surface runoff simulated by the WetSpass model was used to calibrate the model with ground observed streamflow data obtained from the Melkaoda watershed as shown in table 4.3 below.

Table 4. 3: Observed monthly average stream flow data

year	Jan	Feb	Mar	Apr	May	Jun	July	Aug	Sep	Oct	Nov	Dec
1993	0.17	0.26	0.10	0.38	1.75	2.13	4.13	4.27	3.91	4.34	1.18	0.23
1994	0.13	0.10	0.14	0.13	0.22	0.31	5.16	4.25	4.19	1.15	0.23	0.13
1995	0.09	0.10	0.22	0.46	0.72	0.39	1.46	4.08	3.10	0.89	0.21	0.15
1996	0.20	0.07	0.19	0.53	1.14	2.50	2.19	4.55	1.90	1.22	0.28	0.13
1997	0.19	0.05	0.06	0.64	0.32	0.97	3.09	4.28	1.88	2.82	1.41	0.36
1998	0.21	0.10	0.24	0.31	1.06	1.36	2.53	2.66	2.22	4.52	0.83	0.15
1999	0.08	0.05	0.14	0.07	0.09	0.61	2.27	3.40	2.15	2.30	0.52	0.15
2000	0.11	0.07	0.05	0.13	0.18	0.35	1.43	4.19	2.78	3.88	0.69	0.20
2001	0.11	0.10	0.38	0.25	0.40	2.12	3.47	4.44	3.03	1.98	0.38	0.18
2002	0.13	0.06	0.16	0.06	0.25	0.28	4.27	1.77	2.66	1.07	0.20	0.17
2003	0.08	0.05	0.08	0.58	0.44	0.21	1.42	2.34	4.47	2.28	0.52	0.15
2004	0.11	0.07	0.05	0.13	0.18	0.16	4.15	2.03	3.06	3.59	0.28	0.09
2005	0.08	0.04	0.13	0.20	1.20	0.43	1.81	2.25	4.72	1.74	0.40	0.09
2006	0.05	0.08	0.20	1.72	2.19	0.88	3.06	4.16	5.15	1.93	0.48	0.15

Source: Ministry of water, Irrigation and Energy

NSE of 0.89, a correlation of coefficient of determination R^2 of 0.97, and 23 percent of bias were obtained with the parameters of the optimal soil moisture alfa coefficient value of “x” = 9.5, LP = 0.95, interception parameter “a” = 9.5, and a runoff delay factor “x” = 0.9.

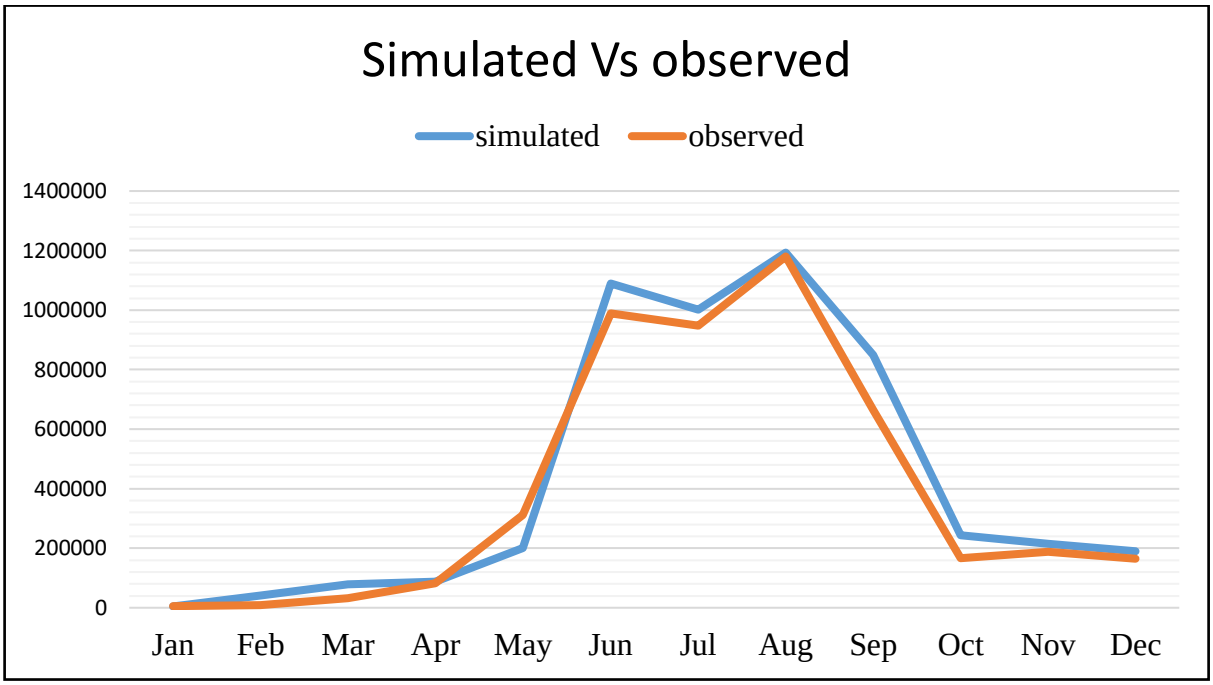

Figure 4. 3: Compression between simulated and observed flow data

4.2.3 Model Outputs

After running the WetSpass model, spatial grid maps of the watershed have been produced monthly. Effective run of WetSpass model produces three main grid maps continuously with one run simulation. Hence, minimum and maximum values of surface runoff, actual evapotranspiration, and recharge were produced for the Melkaoda watershed. The watershed simulated values were unique average values produced from each cell in the watershed as summarized in table 4.4 below. Hence, the following discussions explain the detail of these issues.

Table 4. 4: Simulated monthly water balance components

Months	Water Balance components (2018)		
	Recharge (mm)	Runoff (mm)	AET (mm)
Jan	8.59	7.66	396.02
Feb	13.06	11.89	407.90
Mar	31.39	44.52	1172.02
Apr	33.00	53.03	1276.28
May	32.92	48.48	1365.72
Jun	36.65	87.78	1121.44
Jul	48.43	73.01	1027.53
Aug	64.01	80.42	699.21
Sep	64.50	74.37	750.87
Oct	3.97	52.02	423.40
Nov	16.34	10.30	363.74
Dec	0.45	7.67	369.58

Actual evapotranspiration (AET)

The WetSpass-M model calculated the actual evapotranspiration as a sum of evaporations from the open water bodies, transpiration through vegetated cover, interception loss by vegetation, and evaporation from bare soil. Actual evapotranspiration is a major component of water balance to determine groundwater recharge of the Melkaoda watershed. The result showed that a minimum and maximum value of 363.74mm and 1365.72mm respectively with an average of 781.14mm of water was lost through evapotranspiration in a year from the watershed. On average, this accounts for 81.55% of the watershed's average rainfall (957.8036mm). This is happened due to the high rate of radiation and the dry wind availability as well as the presence of different landuse land covers in the study area. The Melkaoda watershed is mostly covered by different vegetation like agriculture, grassland, and forest. This facilitates evapotranspiration by reducing surface runoff in the watershed.

The WetSpass model simulated the actual evapotranspiration monthly. To get the annual values for the water balance components of the watershed the monthly results have to be summed up from twelve months.

Surface runoff

A spatial long-term average monthly surface runoff simulated by the WetSpass model was presented in table 4.5 above. The model result shows that the annual value of runoff in the Melkaoda watershed varies in the range from 1.24 mm/yr to 87.78 mm/yr as a minimum and maximum values respectively with a mean of 45.93mm/yr. The mean value accounted for about 4.8% of the total annual average rainfall of the watershed. The runoff value was highly dependent on runoff coefficients. The runoff coefficient is also highly influenced by the change in soil moisture, infiltration capacity, landuse/land cover, and the amount and intensity of rainfall, and also the spatial variation of surface runoff value in the watershed is highly dependent on different biophysical factors such as slope.

Groundwater recharge

The amount of infiltration-percolation into groundwater recharge depends on different factors such as slope, landuse, soil texture, and groundwater level (Al Kuisi, M., & El-Naqa, A., 2013). There were different models used to estimate recharge in a given area depending on actual areal conditions.

In this case, the WetSpass-m model estimates the long-term monthly spatiotemporal distribution of groundwater recharge subtracting surface runoff and evapotranspiration from precipitation. The model determined the average monthly groundwater recharge depending on different input variables. The recharge was estimated as the residual of the water balance components from precipitation. Due to this, it responded to variations with varying in different input variables and model parameters. According to the WetSpass result, the annual recharge of the Melkaoda watershed is between 0.45 and 64.5mm /yr as a minimum and maximum value respectively with a mean of 32.47mm/yr. The mean value accounts for about 3.39% of the total annual average rainfall of the watershed.

Recent studies showed that the WetSpass model was implemented in different regions by different authors and their findings showed that their simulation results were acceptable, these

simulation results were stated as follows as cited by (Zarei et al., 2016;Abu-Saleem et al.., 2010), evaluated the water balance components using the WetSpass model for the Hasa basin in Jordan. According to their results, mean annual groundwater recharge and surface runoffs were 0.98 and 23.64 mm/ year, respectively, and about 0.64% and 15.4% recharge and runoff respectively.

In Northern Ethiopia, (Arefaine et al.., 2012) simulated the water balance components including the groundwater recharge, evapotranspiration, and surface runoff using the WetSpass model. Results showed that the mean annual groundwater recharge, evapotranspiration, and surface runoff were found to be 12% of the precipitation becomes recharge while evapotranspiration and surface runoff are 81% and 7% of the precipitation, respectively and (Esayas and Gebeyehu, 2018) have reported that The total mean annual rainfall of the watershed contributes to 7.4% as recharge to groundwater, 7.1% of surface runoff and 85.5% of evapotranspiration.

Accordingly, an average recharge of 0.27 mm, 0.5% of precipitation (Mustafa Al Kuisi and Ali El-Naqa, 2013): recharge of 28 mm, 5% of annual precipitation (Tilahun and Merkel. 2009) and 37 mm, 6% of precipitation (Tesfamichael et al.., 2010). (Gebremeskel, 2015) has reported that groundwater recharge was 4.2% of the annual precipitation. According to the above different scholar's results, the WetSpass model simulated the water balance components in the Melkaoda watershed which is 3.4% as recharge to groundwater, 4.8% surface runoff, and 81.8% evapotranspiration have similarity with results shown above. Therefore, it could be said that the WetSpass model has worked well in Melkaoda watershed and has simulated hydrological water balance components efficiently.

4.3 Impact of landuse change on groundwater recharge

4.3.1 Model output

Again after running the WetSpass model for the two images separately, spatial grid maps of the watershed have produced monthly. Effective run of WetSpass model produces three main grid maps continuously with one run simulation.

Table 4. 5: The model result of water balance components in 1989 and 2018.

Months	Water Balance components (2018)			Water Balance components (1989)		
	Recharge	Runoff	AET	Recharge	Runoff	AET
Jan	2.45	1.24	396.02	43.1	3.41	341.5
Feb	13.06	11.89	407.90	13.8	7.72	354.7
Mar	31.39	44.52	1172.02	31.4	27.98	1071.4
Apr	33.00	53.03	1276.28	36.9	33.50	1149.3
May	3.92	48.48	1365.72	37.1	28.45	1247.8
Jun	32.97	87.78	1121.44	33.0	79.07	914.4
Jul	48.43	73.01	1027.53	88.4	70.32	921.0
Aug	64.01	80.42	699.21	57.6	86.94	685.6
Sep	64.50	74.37	750.87	55.4	81.59	738.1
Oct	36.65	52.02	423.40	32.4	53.86	411.8
Nov	16.34	10.30	363.74	17.4	9.74	322.6
Dec	0.45	1.85	369.58	8.0	3.29	316.5

Long-term monthly average groundwater recharge under the landuse conditions in 1989 and 2018 was also simulated to quantify differences due to changes in landuse from 1989 to 2018. Therefore, the results reflect the impact of landuse changes on the groundwater recharge in the Melkaoda watershed from 1989 to 2018. The watershed-wide and spatially average simulated water balance components of the study area are shown in Table 4.4 above. The mean annual groundwater recharge rate was 38 mm/yr and 32.47 mm/yr for 1989 and 2018, respectively. Recharge accounted for 3.9 to 3.4% in 1989 and 2018 respectively of the precipitation. The vegetation covers such as forest land and grassland which promote the groundwater recharge and prohibited the surface runoff and actual evapotranspiration are decreasing by 0.602 and 1.78 rates per year respectively from 1989 to 2018 and also the bare land that prohibits the groundwater recharge is also decreasing by 1.87 rates per a year. But the agricultural land and built-up area have been increasing by 0.046 and 2.56 rate respectively per a year. The increment of built-up area and decreasing of forest land grassland in the Melkaoada watershed leads to a decrease in groundwater recharge. Urban land, which has increased in response to urbanization and expansion of rural settlements, results in a decrease in recharge.

In other research the result indicated urban land that to be considered as impervious areas promote surface runoff and prohibit infiltration (Jat et al.., 2009), and as most of the water from precipitation is lost in the form of evaporation, vegetation cover becomes an important parameter regulating the recharge rate (Lin et al., 2010).

5. SUMMARY AND CONCLUSION

5.1 Summary

The water resource is a critical aspect to sustain life and it should be investigated and understand the hydrological environment for planning, managing, and proper utilization of water resource. Nowadays. Surface water use is decreasing due to different reasons like contamination and pollution that leading the water resource concentration to groundwater. For groundwater potential zone mapping, eight parameters were selected which affect more the occurrence of groundwater potential zone before overlay analysis. By assigning quantitative weights, it is possible to make important criteria that have a greater influence on the result than other criteria. For this task, AHP approach was adapted and give the value for each factor. This approach allows decision-makers to give judgments to reduce complexity in decision-making processes. It focused on the integration of Remote Sensing and GIS technologies in the identification and delineation of groundwater potential zones in the Melkaoda watershed. The remote sensing and GIS was a potentially effective tool and Very useful in the delineation of groundwater potential zones.

The result shows that most of the very high potential areas represented by plains, low drainage density, very high rainfall, (Nn) geological formation that highly permeable, coincide with the low slope and finally the result indicates the watershed was identified and delineated in four categories namely very high, high, low and very low and the majority of the area is covered by high potential zones as it is supported by the statistical data of groundwater borehole wells and the new predicted groundwater potential map of the study area.

Model validation of predicted groundwater potential zones with the groundwater borehole wells data shows 100% with total borehole wells were correctly agreed with predicted groundwater potential zones.

There are different physical and empirical models to understand the water balance components of a given watershed. One of the spatially distributed physical models is the WetSpass-m model. The model considers all meteorological, hydrological, and biophysical factors of the area to evaluate groundwater recharge and other water balance components of the watershed. The WetSpass-M model has simulated the water balance components of the Melkaoda watershed successfully.

The highly variable distribution of the climatic inputs (parameters) associated with variation of landuse/land cover, soil texture, topography, and slope are responsible for variations of the water balance element within the watershed. Based on the model, the annual groundwater recharge in the Melkaoda watershed is 0.45 and 64.5mm/yr as a minimum and maximum value with a mean of 32.47mm/yr. This represents 3.4% of the total annual rainfall.

The annual rainfall is distributed to different water balance components in the Melkaoda watershed. From this, most of the rainfall amount is back to the hydrological cycle through evapotranspiration, and remaining part is distributed as runoff and groundwater recharge. Topographically high elevated areas which are located in the upper part of the watershed in combination with natural forests have high groundwater recharges.

With the landuse changing from 1989 to 2018, the annual groundwater recharge in the study area has decreasing from time to time. The decrease of cropland and grassland together with the increase of urban area and rural settlements are the major reasons.

5.2 Conclusion

Different factors govern the occurrence, movement, and storage of groundwater. For the mapping of groundwater zone, all factors were considered and they were slope, geology, drainage density, lineament density, landforms, LULC, rainfall, and soil. ArcGIS technology was used for the thematic map preparation of each governing factor. After preparation of thematic maps reclassification and overlay analysis with AHP process is done to classify the study area into the different potential zone and the result shown divide the area into four groundwater potential zone such as very low, low, high, and very high and validation result was also indicates that the classified zone has a good agreement with the (JMG, 2007) groundwater potential zone classification. The water balance components of the vegetated area, bare-soil, open-water bodies, and impervious land surfaces are used to compute the total water balance of a raster cell for a given watershed using the WetSpass-M model and the total evapotranspiration, surface runoff, and groundwater recharge of a raster cell was calculated. For this calculation generally, two types of data such as meteor-hydrological and spatial data were used. Comparing the model result with the results obtained by different researchers in different areas the model showed good agreement with the study area.

The impacts of LULC changes on groundwater potential is also assessed in the study area using this model by taking the two image of different years that means 1989 and 2018 satellite images. The result shown that three of LULC parameters were decreased and two of LULC were increased including built-up area and the urban land promotes surface runoff and decreases groundwater recharges.

Recommendation

Information on the delineation of the groundwater potential zone will be useful for effective identification of the suitable locations for extraction of groundwater, planners, engineers, and decision-makers and used as a guideline for further research. As the result of groundwater potential zone mapping shown that all boreholes are felt in a high groundwater potential zone but to get much water they have to drill wells from the area of a very high groundwater potential zone.

The results obtained from the WetSpass model in this study can be taken as an initial investigation in the groundwater recharge modeling of the Melkaoda watershed. The groundwater recharge and other water balance components result can be improved further and reached to more accurate if more monitored monthly groundwater depth data, new and sufficient borehole data, and landuse data that is prepared in fine resolution and new meteorological stations become available at the watershed. Because the graphical user interface WetSpass model is highly sensitive to those input data.

From the result of the impacts of LULC changes on the groundwater recharges urbanization was increasing at a rapid rate and forest area, grassland, and bare land were decreasing. If this condition to be continued the area would get very little amount or total loss of the groundwater potential. So to save the groundwater of the area community and government should focus on planting the tree on bare land and promote urban agriculture in the area and they have to promote agriculture. In addition to these, an artificial recharge has be encouraged.

REFERENCES

Abdollahi, K., Bashir, I., Verbeiren, B., Mahamane, H. R., Van Griensven, A., Huysmans M., & Batelaan, O. (2017). A distributed monthly wayer balance model. *formulation and application on Black Volta Basin Environ Earth Sci (2017)*, 76-198.

Abdollahi, K., Bashir, I., Verbeiren, B., Mahamane, H. R., Van Griensven, A., Huysmans,. (2017). A distributed monthly water balance. *formulation and application on Black Volta Basin Environ Earth Science*, 76-198.

Abdullahi, J., Momoh, E., Udensi. (2013). Effect of Lineaments on Groundwater Occurrence. *Int J Environ Bioenergy*, 22-32.

Abu-Saleem A, Al-Zu`bi Y, Rimawi O, Al-Zu`bi J, Alouran N. (2010). Estimation of water balance components in the Hasa basin with GIS based WetSpass model. *J Agron 9(3):*, 119–125.

Adnan M. Aish, O. Batelaan, F. De Smedt. (2010). Distributed Recharge Estimation For Groundwater Modeling Using Wetspass Model, Case Study - Gaza Strip, Palestine. *The Arabian Journal for Science and Engineering, Volume 35, Number 1B* , 155.

Aduah, M. (2015). Analysis Of Land Cover Changes in the Bonsa Catchment, Ankobra Basin, Ghana. *Appl. Ecol. Environ. Res. 13:*, 935–955.

Aish, A. M. (2009). Estimation of water balance components in the Gaza Strip with GIS-based. *Environ Earth Sci.*, 54-68.

Al Kuisi, M., & El-Naqa, A. (2013). GIS based spatial groundwater recharge estimation in the Jafar basin, Jorda. *Application of WetSpass models for arid regions*, 96-109.

Annesh and Paresh. (2015). High Resolution Groundwater Prospect Mapping of Raichur, Karnataka using Remote Sensing and GIS. *Imperial Journal of Interdisciplinary Research, 2(8)*.

Arefaine Teklebirhan, Dessie Nedaw and Tesfamichael Gebreyohannes. (2012). Groundwater Recharge, Evapotranspiration and Surface Runoff Estimation Using WetSpass Modeling Method in Illala Catchment, Northern Ethiopia . *Momona Ethiopian Journal of Science (MEJS),* , V4 (2):96-110.

Arefayne Shishaye H, Abdi S . (2015). Groundwater exploration for water well site locations using geophysical survey methods. *J Waste Water Treat Anal 7(1)*, 1-7.

Arivalagan, S. (2014). Delineation of groundwater potential zones using RS and GIS techniques: a case study for Eastern part of Krishnagiri district, Tamil Nadu. *International Journal of Advance Research in Science and Engineering*, 3(3):51-59.

Arnot, R.H. & Grant, K. (1981). The application of a method for terrain analysis to functional land-capability assessment and aesthetic landscape appreciation. *Landscape Planning 8:*, 269-300.

Azita Ahmad Zawawi*, Masami Shiba & Noor Janatun Naim Jemali. (2014). Landform Classifcation for Site Evaluation and Forest Planning: Integration between Scientifc Approach and Traditional Concept. *Sains Malaysiana 43(3)*, 349–358.

B., B. (2014). Surface Water and Groundwater Resources of Ethiopia Potentials and Challenges of Water Resources Development. *Springer International Switzerland*, 106.

Batelaan O. and S.T. Woldeamlak. (2007). rcView Interface for WetSpass, User Manual,Version 13-06-2007. *Vrije Universiteit, Hydrology and Hydraulic Engineering,Brussels.*

Batelaan, O., & DeSmedt, F. (2001). WetSpass: a Flexible, GIS Based, Distributed Recharge Methodology for Regional Groundwater Modelling. *IAHS Publ. no. 269*, 76-98.

Batelaan, O; De Semdt, F. . (2007). GIS based recharge estimation by coupling surface-subsurface water balances. *IAHS*, 78-86.

Beven, K. (2000). Rainfall-Runoff Modeling. *The Primer, John Wiley & Sons, Ltd., New York*.

Bonansea, M. (2016). Assessing the impact of land use and land cover on water quaity in the watershed of a reservoir. *Appl. Ecol. Environ. Res. 14*, 447–456.

Caetano, M., Mata, F., Freire, S. (2005). Accuracy Assessment of the Portuguese corine. *Global Developments in environmental earth observation*, 459-467.

Charles, R. (2002). Groundwater science an important of elsevier science. *San Diago, California*, 2101-4495.

Craig, C., Rick, E., Susan, H., Rafik, H., Gabrielle, P., & Carolina, P. . (2010). Water and climate change: impacts on groundwater resources and adaptaion options. *Water working nots.*, 250-365.

Daniel Alemayehu, Meseret Tadesse, Mohammed Abdul Athick AS. (2018). Application of TPI for analysis of landforms and LULCof Adama woreda, Ethiopia. *J. Geographical Studies, 2(2),*, 100-109.

Dinesh Kumar PK, G. G. (2007). Application of remote sensing and GIS for the demarcation of groundwater potential zones of a river basin in Kerala, southwest cost of India. *Internaltional Journal Remote Sensing*, 5583–5601.

E.Obuobie, W. Agyekum, B. Diekkrueger, and S. Agodzo, S,. (2012). Groundwater level monitoring and recharge estimation in the White Volta River basin of Ghana. *Journal of African Earth Sciences,*, volume 71-72: 80–86.

Esayas Meresa and Gebeyehu Taye. (2018). Estimation of groundwater recharge using GIS-based WetSpass model for Birki watershed, the eastern zone of Tigray, Northern Ethiopia. *Springer*, 1555–1566.

FAO. (2006). *Guidelines for soil description.* Rome: Viale delle Terme di Caracalla, 00100 Rome, Italy.

Fenta AA, Kifle A, Gebreyohannes T, Hailu G. (2014). Spatial analysis of groundwater potential using remote sensing and GISbased multi-criteria evaluation in Raya Valley, northern Ethiopia. *Hydrogeol J 23(1*, 195–206.

Foody, G. M. (2002). Status of land cover classification accuracy assessment. *Remote Sensing Environmental*, 185–201.

Freeze, A. R. (1969). The Mechanism of Natural Groundwater Recharge and Discharge, One-Dimensional, Vertical Unsteady, Unsaturated Flow Above a Recharging or Discharging Groundwater Flow System". *Wat. Resour.Res., 5(1)*, 153–171.

Giordano, M. (2009). Global Groundwater? Issues and Solutions. *International Water Management Institute*, 34:153–78.

Gupta, R. P. (2003). Remote Sensing Geology". 2nd ed. Springer, Berlin, Germany. *International Journal of Innovational Sciience*, 460-477.

Gurnell, A.M., Corenblit, D., García de Jalón, D., González del Tánago, M., Grabowski R.C., O'Hare, M.T., Szewczyk, M. . (2016). A Conceptual Model of Vegetation hydrogeomorphology Interactions Within River Corridors. *River Res. Appl. 32*, 142-163.

HAILE, G. G. (2015). Estimation Of Groundwater Recharge And Potentials Msc Thesis. *Haramaya University, Haramaya*, 81.

Hobbs, W. (1904). Lineaments of the Atlantic Border Region. *Geological Society. American Bulletin,15,* 483-506.

Hornsby, A. G. (1986). A microcomputer-based management tool for chemical movement in soil. *Applied agricultural research*, 1(1), 50-56.

Hornsby,Maurice D.R.. and Courteny. (1990). Micro computer-baesd management tool for chemical movement in soil, the physics of mechanical alloying a first repot. *Applied agricultural research, Metallurgical transaction*, 1(1),50-56 and 21(1),289-303.

Hsi-Fuyeh, C.-H.-C. (2016). GIS for assessment of groundwater recharge potential zone. *Environmental Geology*, 58:185-195.

Jinno, K., Tsutsumi, A., Alkaeed, O., Saita, S., Berndtsson, R. (2009). Effects of land-use change on groundwater recharge model parameters. *Hydrol. Sci. J. 54:*, 300–315.

JMG. (2007). Hydrogeological map of Selangor and Kuala Lumpur. *Federal Territory*.

K. Abdollahi, I. Bashir and O. Batelaan. (2012). WetSpass Graphical User Interface. *Vrije Universiteit BrusseL Version 31-05-2012*.

KA, M. (2000). Groundwater prediction potential zone in Langat Basin using the integration of remote sensing and GIS. *Retrieved July 24, 2000, from http://www.gisdevelopment.net*.

Kavitha, M., Mohana, P., and Naidu, K.B. (2011). elineating groundwater potential zones in Thurinjapuram watershed using geospatial techniques. *Indian Journal of Science and Technology*, 4 (11), 1470–1476.

Kebede, S. (2010). Groundwater in Ethiopia Occurrence, drought proofing and technology options.

Kohler, T. & Breu, T. (2005). GIS based watershed classifcation in the Lower Mekong Basin. Watershed Classifcation Project. *Vietnam Center for Development and Environment.*

Krishnamurthy, J. A. (1995). Role of geological and geomorphological factors in ground water exploration: a study using IRS LISS data. *International Journal of Remote Sensing*, 2595-2618.

Krishnamurthy, J. and Srinivas, G. (1995). Role of geological and geomorphological exploration – a study through remote sensing techniques. *Int. Jour. Remote Sensing, Vol. 16,*, 2595-2618.

Lerner DN, Harris B . (2009). The relationship between land use and groundwater resources and quality. *Land Use Policy 26*, S265–S273.

Lin, H.S., Flühler, H., Otten, W., and Vogel, H.J. (2010). Soil Architecture and Preferential Flow across Scales. *Journal of Hydrology*, 393:1-2.

M. Zeinolabedinia, A. Esmaeily. (2015). Groundwater Potential Assessment Using Geographic Information Systems And Ahp Method (Case Study: Baft City, Kerman, Iran). *The International Archives of the Photogrammetry*, 769.

M.L.Waikar1 and Aditya P. Nilawar. (2014). Identification of Groundwater Potential Zone using Remote Sensing and GIS Technique. *International Journal of Innovative Research in Science,Engineering and Technology*, 12163.

Malczewski, J. (1999). GIS and multicriteria decision analysis. *New York, Wiley*.

Manandhar, R., Odeh, I. And Ancev, T. (2009). Improving The Accuracy of Land Use and Land Cover Classification of Landsat Data Using Post-Classification Enhancement. *Journal of Remote sensing*, 330-344.

Manap, M. (2013). A knowledge-driven GIS modeling technique for groundwater potential mapping at the Upper Langat Basin, Malaysia. *Arabian Journal of Geosciences*, 6(5),1621–1637.

Mata-González, R., McLendon, T., Martin, D.W., Trlica, M.J., Pearce, R.A. (2012). Vegetation as affected by groundwater depth and microtopography in a shallow aquifer area of the Great Basin. *Ecohydrology 5*, 54–63.

Maurice, D. R., and Courtney, T. H. . (1990). The physics of mechanical alloying: a first Repot. *Metallurgical Transactions*, 21(1), 289-303.

Morelli, M., and Piana, F. (2006). Comparison between remote sensed lineaments and geological structures in intensively cultivated hills (Monferrato and Langhe domains, NW Italy . *International Journal of Remote Sensing, 27(20)*, 4471-4493.

Morris BL, Lawrence AR, Stuart ME. (1994). *The impact of urbanisation on groundwater quality (project summary report).* Nottingham, UK: British Geological Survery.

Mukherje, A. (2008). Deeper groundwater chemistry and geochemical modeling of the arsenic affected western Bengal basin,West Bengal, India . *Applied Geochemistry, 23(4)*, 863-894.

Murugesan B, Thirunavukkarasu R, Senapathi V, Balasubramanian G. (2012). Application of remote sensing and GIS analysis for groundwater potential zone in kodaikanal Taluka, South India. *Earth Sci. 7(1),* 65-75.

Mustafa Al Kuisi and Ali El-Naqa. (2013). GIS based Spatial Groundwater Recharge estimation in the Jafr basin, Jordan – Application of WetSpass models for arid regions. *Rivista Mexicana de Ciencias Geológicas*, 30 (1): 96-109.

N.D., M. (2007). Model Evaluation Guide Line for Systematic Quantification of Accuracy in Watershed Simulations. *American Society of Agriculture and Biological*.

Nilawar P. & Waikar M.L. (2014). Identification of Groundwater Potential Zone using Remote Sensing and GIS Technique. *International Journal of Innovative Research in Science*.

On., S. (1786). An English translation of the Sanrin Shinpi. *Scientifc Bulletin of the Faculty of Agriculture*.

Panda, D.K., Kumar, A. . (2011). Evaluation of an over-used coastal aquifer (Orissa, India) using statistical approaches. *Hydrol. Sci. J.56;*, 486–497.

Pistocchi, A., Bouraoui, F., & Bittelli, M. (2008). A simplified parametrization of the monthly top soil water budget. *Journal of Hydrology*, 44-63.

Prasad, R. M. (2008). Deciphering potential groundwater zone in hard rock through the application GIS. *Environmental Geology*, vol. 55, pp. 467–475.

Raghunath. (2006). Hydrology principles analysis and design revised second edition. *Springer*, 135 - 154.

Rahmati, O. (2015). Groundwater potential mapping at Kurdistan region of Iran using analytic hierarchy process and GIS. *Arabian Journal of Geosciences*, 8(9), 7059–7071.

Rai B, T. A. (2008). Identification of groundwater prospective zones using remote sensing and geoelectrical methods in Jharia and Raniganj coalfields, Dhanbad district, Jharkhand state. *J Earth Syst Sci, 114(5)*, 515–522.

Ramu & vinay. (2014). Site Suitability Analysis for Artificial recharge. *International Journal of Advanced Research in Science and Technology*.

Rashman. (2016). Identification of Groundwater recharge potential zones in Thiruverumbur block,.

Ricca, N., Guagliardi, I. (2015). Multi-temporal dynamics of land use patterns in a site of community importance in southern Italy. *Appl Ecol Env. Res. 13*, 677–691.

Rwanga, S. S. (2013). A Review on Groundwater Recharge Estimation Using Wetspass Model. *International Conference on Civil and Environmental Engineering* (p. 156). Johannesburg (South Africa): CEE.

S. Stoll. (2012). On the impact of climate change on Groundwater resources PhD Thesis, DISS. *ETH NO. 20443, Eth Zurich*.

Saaty, T. (1980)). Marketing applications of the analytic hierarchy process. *Management science*, 26(7), 641-658.

Saaty, T. (2008). Decision Making with the Analytic Hierarchy Process. *International Journal of Services Sciences*, 1, 83.

Saaty, T. L. (1980). *The Analytic Hierarchy Process.* New York: McGraw-Hill.

Salvadore E, Bronders J, Batelaan O. (2015). Hydrological modelling of urbanized catchments: a review and future directions. *J Hydrol*, 529:62–81.

Salwa, F. (2015). An overview of integrated remote sensing and GIS for groundwater mapping in Egypt. *Ain Shams Engineering Journal, 6(1)*, 1-15.

Santhi J. G. Arnold J. R. Williams W. A. Dugas R. Srinivasan L. M. Hauck. (2001). Validation Of The Swat Model On A Large Rwer Basin With Point And Nonpoint Sources. *Journal of the American Water Resources Association*, 1169-1188.

Schirmer M, Leschik S, Musolff A. (2013). Current research in urban hydrogeology—a review. *Adv Water Resour 51*, 280–291.

Semere, S. (2003). Remote sensing and GIS:applications for groundwater potential assessment in .

Shaban A, K. M. (2006). Use of remote sensing and GIS to determine recharge potential zones the case of Occidental Lebanon. *Hydrogeol Journal*, 433–443.

Shanableh A, Merabtene T . (2015). Geomatics for mapping of groundwater potential zones in the northern part of the United Arab Emiratis—Sharjah City. . *Sens Spatial Inf Sci*.

Shifaji, G., Shifaji, P., Nitin, M. (2014). Identification of groundwater recharge potential zones for a watershed using remote sensing and GIS. *International Journal of Geomatics and Geosciences*, 4(3), 485-498.

Stafano Carnicelli,C.Lasio,Serena di Grazia and Datro Ventra G.A. Ferrari , C. Iasio , M. Sagri , D. Ventra , Balemwald Atnafu , Seifu Kebede. (2002). The Ziway–Shala lake basin (main Ethiopian rift, Ethiopia): a revision of basin evolution with special reference to the Late Quaternary . *Journal of African Earth Science*.

Subramanya, K. (2008). *Engineering Hydrology Book, Third Edition, Former Professor of Civil Engineering Indian Institute of Technology Kanpur,.* Tata: Tata Mcgraw-Hill Publishing Company, Pp 29-51.

T, A. (1998). The hydrogeological system of the Lake District basin, Central Main Ethiopian Rift. *The Netherlands,Free University of Amsterdam*, 259.

T. L. Saaty and L. G. Vargas,. (1981). *The Logic of Priorities, Applications in Bu,sines.., energy, Health, Transportation. .* The Hague: Nijhoff.

T., A. (1998). The hydrogeological system of the Lake District basin, Central Main Ethiopian Rift. *The Netherlands; Free University of Amsterdam*, 259.

Tamiru. (2006). Groundwater occurrence in Ethiopia. Addis Ababa University, Ethiopia. *With the*.

Tesfa Gebrie Andualema,∗, Girum Getachew Demeke. (2019). Groundwater potential assessment using GIS and remote sensing: A case study of Guna tana landscape, upper blue Nile Basin, Ethiopia. *Journal of Hydrology: Regional Studies*.

Tesfamichael G., De Smedt F., Miruts H., Solomon G., Kassa A., Kurkura K., Abdulwassie H., Bauer H., Nyssen J., Moeyersons J., Deckers J., Mitiku H. and Nurhussen T . (2010). Large-scale geological mapping of the Geba basin, northern Ethiopia. *VLIR – Mekelle University IUC Program*, 46 pp. ISBN 978-90-8826-134-3.

Tesfaye, T. (2010). Groundwater Potential Evaluation Based on Integrated GIS and Remote sensing techniques, in Bilate River Catchment, South Rift Valley of Ethiopia. *Addis Ababa, Ethiopia.*

Tesfaye, T. (2012). Ground water potential evaluation based on integrated GIS and remote sensing techniques, in bilate river catchment: south rift valley of Ethiopia (AAU) .

Tetzlaff D, Soulsby C, Bacon P, Youngson A, Gibbins C, Malcolm I. (2007). Connectivity between landscapes and riverscapes—a unifying theme in integrating hydrology and ecology in catchment science :. *Hydrol Process 21(10)*, 1385–1389.

Thangarajan., M. (2007). Groundwater Resource Evaluation, Augmentation, Contamination,Restoration, Modeling and Management.

Tilahun Ketema and Broder J. Merkel. (2009). Estimation of groundwater recharge using a GIS based distributed water balance model in Dire Dawa, Ethiopia. *Hydrogeology Journal,*, 17: 1443–1457.

Tolche, A. D. (2021). Groundwater potential mapping using geospatial techniques: a case study of Dhungeta-Ramis sub basin, Ethiopia. *Geology, Ecology, and Landscapes*, 65-80.

UNEP. (2010). In A. W.Atlas, Division of Early Warning and Assessment (DEWA). Nairobi,. *United Nations Environment Programme (UNEP)*.

Waikar, A. a. (may,2014). identification of grundwater potential zone. *International Journal of rechearch in science*, 63-74.

Y, F. (2015). Groundwater in the Earth's critical zone—relevance to large-scale patterns and processes. . *Water Resour Res 51(5)*, 3052–3069.

Zarei M, Ghazavi R, Vli A, Abdollahi K. (2016). Estimating groundwater recharge, evapotranspiration and surface runoff using land-use data:a case study in northeast Iran. *Biol Forum 8(2*, 196–202.

Zomlot Z, Verbeiren B, Huysmans M, Batelaan O . (2015). Regional studies spatial distribution of groundwater recharge and base flow. Assessment of controlling factors. . *J Hydrol 4:*, 349–368.

APPENDICES

Appendix 7. 1:Long-term average monthly wind speed of three stations in and around the study area.

station	Jan	Feb	Mar	Apr	May	Jun	Jul	Aug	Sep	Oct	Nov	Dec	annual (m/s)	avg.monthly(m/s)
shashemene	1.090	1.138	1.124	1.063	1.046	1.248	1.233	1.150	0.929	0.964	1.030	1.066	13.082	1.090
kuyera	1.095	1.143	1.129	1.068	1.051	1.253	1.238	1.154	0.934	0.969	1.035	1.070	13.140	1.095
kofele	1.270	1.338	1.308	1.291	1.178	1.350	1.401	1.313	1.082	1.211	1.276	1.267	15.285	1.274

Source: National Meteorological Agency of Ethiopia

Appendix 7. 2:Long-term average monthly groundwater depth (m) of three stations in and around the study area.

Well Name	Jan	Feb	Mar	Apr	May	Jun	Jul	Aug	Sep	Oct	Nov	Dec	Avg.depth
Alelu Ilu	180	180	180	180	180	180	180	180	180	180	180	180	180
Shire Borara	159	159	159	159	159	159	159	159	159	159	159	159	159
Awasho Dinku #3	311	311	311	311	311	311	311	311	311	311	311	311	311
Awasho Dinku #4	277	277	277	277	277	277	277	277	277	277	277	277	277
Faji sole	168.6	168.6	168.6	168.6	168.6	168.6	168.6	168.6	168.6	168.6	168.6	168.6	168.6
Bute Filicha	164.25	164.25	164.25	164.25	164.25	164.25	164.25	164.25	164.25	164.25	164.25	164.25	164.25

Source: West Arsi Zone water, mineral and energy office

Appendix 7. 3:Long-term average monthly temperature of three stations in and around the study area.

station	Jan	Feb	Mar	Apr	May	Jun	Jul	Aug	Sep	Oct	Nov	Dec	Annual	avg annual
shashemene	24.79	26.39	26.54	25.41	24.47	23.31	22.26	22.36	23.18	24.08	24.89	24.77	292.44	24.37
Kuyera	26.07	27.52	28.08	27.39	26.88	25.66	23.87	24.00	24.98	25.94	26.20	25.90	312.50	26.04
kofele	20.61	21.84	22.04	20.56	20.09	18.76	17.70	17.92	18.65	19.16	19.82	20.03	237.18	19.76

Appendix 7. 4: Long term average monthly rainfall (mm) of three stations in and around the study area

Station	Jan	Feb	Mar	Apr	may	Jun	Jul	Aug	Sep	Oc	No	De	Annual	normal
shahemene	552.9	795.6	1820.7	2982.5	1894.7	2777	2655.8	3030.4	2515.25	1802.8	611.4	518.	21957.	731.91
Kuyera	462.7	1091.4	1776.7	2675.5	2311.6	3443.2	3642.6	3674.2	3394.5	1615.1	457.6	374.	24919.	830.6
Kofele	1138	1324	3731	4119	3673	4027	4289	4533	4394	2950	1407	1052.	36642.	1221.

Source: National Meteorological Agency of Ethiopia

Appendix 7. 5: Landuse/cover lookup parameter table

Code	LUSE_TYPE	RUNOFF_VEG	VEG_AREA	BARE_AREA	IMP_AREA	OPENW_AREA	ROOT_DEPTH	LAI	MIN_STOM	VEG_HEIGHT	nManing	Land Factor	Aerodyn Resistance
2	build-up	grass	0.5	0	0.5	0	0.3	2	100	0.12	0.04	0.5	212.01
7	barea land	bare soil	0	1	0	0	0.05	0	110	0.001	0.09	0.222	426.67
21	agriculture	crop	0.8	0.2	0	0	0.4	4	180	0.6	0.037	0.541	115.01
33	forest	forest	1	0	0	0	2	5	375	16	0.1	0.2	28.10
307	grass land	grass	1	0	0	0	0.3	2	140	0.12	0.035	0.571	212.01

Appendix 7. 6: Soil parameter lookup table

ID	SOIL	FIELDCAPAC	WILTINGPNT	PAW	RESIDUALWC	A1	EVAPODEPTH	TENSIONHHT	P_FRAC_SUM	P_FRAC_WIN	Teta
12	clay	0.46	0.33	0.13	0.09	0.21	0.05	0.37	0.95	0.85	0.852
5	loam	0.25	0.12	0.13	0.027	0.37	0.05	0.11	0.15	0.02	0.333
7	sandy clayl	0.26	0.16	0.1	0.068	0.32	0.05	0.28	0.54	0.3	0.351
3	sandy loam	0.21	0.09	0.12	0.041	0.44	0.05	0.15	0.09	0.01	0.266

Soil table attributes

Number = Soil type number; Soil = Soil type (texture); Fieldcapac = Field capacity; Wiltingpnt = Wilting Point; PAW = Plant available water content; Residual = Residual water content; A1 = Calibration parameter dependent on the sand content of the soil; Evapodepth = Bare soil evaporation depth; Tensionsh = Tension saturated height; Pfrac_sum = Fraction of summer precipitation contributing to Hortonian runoff; P_frac_win = Fraction of winter precipitation contributing to Hortonian runoff

Appendix 7. 7: Four months rainy days in the Melkaoda watershed

Code	Rainy Days	Code	Rainy Days
1	3	25	6
2	2	26	9
3	1	27	8
4	4	28	14
5	5	29	12
6	17	30	4
7	12	31	7
8	14	32	10
9	8	33	9
10	12	34	12
11	4	35	15
12	9	36	18
13	10	37	19
14	11	38	11
15	14	39	2
16	3	40	3
17	4	41	4
18	1	42	1
19	10	43	4
20	6	44	7
21	5	45	5
22	2	46	14
23	3	47	14
24	7	48	19

Appendix 7. 8: Simulated monthly stream flow data (m3/month)

Months	Qsurf[m³/month]	Qb[m³/month]	Qsurf[m³/month]+ Qb(m3/month)
Jan	1813.464421	2614.491045	4427.955466
Feb	5570.090736	4725.170223	10295.26096
Mar	14591.6002	23580.7502	38172.35039
Apr	30261.96194	36539.21819	66801.18013
May	41399.13061	45976.21846	87375.34907
Jun	73981.19665	38117.41048	112098.6071
Jul	107347.2801	38757.94664	146105.2267
Aug	138332.1461	54873.71064	193205.8567
Sep	167847.6726	70983.46813	238831.1407
Oct	177311.685	65389.89805	242701.5831
Nov	162410.2959	52698.58323	215108.8792
Dec	147936.3728	41994.13284	189930.5057

Appendix 7. 9: Boreholes data from Shashemene water supply bureau

Site Name/kebele		Alelu Ilu	Shire Borara	Awasho Danku BH#3	Awasho Danku BH#4	Faji sole	Bute Filicha
Location (UTM,adindan, m)	x	455464	456920	462737	462146	461617	462294
	y	800180	792615	795210	795570	792336	797560
	z	1853	1997	2098	2084	2154	2062
Target depth(m)		250	350	350	350	350	350
Drilling method		Air rotary & mud	Air rotary	Air rotary	Air rotary	Air rotary	Air rotary
				& mud	& mud	& mud	
ground surface level(m)		270	325	400	356	271	235
Water strike(m)		66-68	170	90-120	75	110	90
Casing(inch)		65/8	6	0+1-200m, 10 200-356m,8	0+1-200m, 10 200-356m,8	8	8
Casing type		Steel	Steel	steel	steel	steel	steel
Screen length(m)		72	93	138.7	119	96	68.64
Static water level(m)		90	166	89	79	102.4	70.75
Discharge(L/s)		2.86	1.86	2.95	5	5	4.8
Dynamic water level(m)		114	188	94.9	86.5	147.2	87.4
Water quality(F)WHO(1.5)		0.89	acceptable	0.41	0.82	< 1.5	< 1.5

Source: West Arsi zone water Mineral and energy office